2019

Development, installation and preliminary data collection of an environmental sensor system for freeze–thaw monitoring under granular-surfaced roadways

Derya Genc
Iowa State University

Development, installation and preliminary data collection of an environmental sensor system for freeze–thaw monitoring under granular-surfaced roadways

by

Derya Genc

A thesis submitted to the graduate faculty

in partial fulfillment of the requirements for the degree of

MASTER OF SCIENCE

Major: Civil Engineering (Geotechnical Engineering)

Program of Study Committee:
Jeramy C. Ashlock, Co-major Professor
Bora Cetin, Co-major Professor
Kristen S. Cetin

The student author, whose presentation of the scholarship herein was approved by the program of study committee, is solely responsible for the content of this thesis. The Graduate College will ensure this thesis is globally accessible and will not permit alterations after a degree is conferred.

Iowa State University

Ames, Iowa

2019

This work is dedicated to my beautiful mom *Deniz Atay*,

none of this would have been possible without you, your unfailing support and unconditional love.

This work is also dedicated to my beloved grandfather *Nevzat Kaya Atay*,

I miss you every day…

TABLE OF CONTENTS

Page

LIST OF FIGURES

Page

NOMENCLATURE

DAQ	Data Acquisition
DE	Differential-Ended
DOT	Department of Transportation
EICM	Enhanced Integrated Climate Model
ESS	Environmental Sensor Station
GPR	Ground Penetrating Radar
mV	Millivolt
PVC	Polyvinyl Chloride
RWIS	Road Weather Information System
SE	Single-Ended
SLR	Spring Load Restrictions
TDR	Time Domain Reflectometry
UV	Ultraviolet
VWC	Volumetric Water Content

ACKNOWLEDGEMENTS

First of all, I would like to thank my major professors Dr. Jeramy Ashlock and Dr. Bora Cetin for their guidance, support and patience throughout my graduate studies. I also would like to thank my committee member Dr. Kristen Cetin for her support and willingness to work with me. I would like to acknowledge and thank Paul Kremer for guiding me and supporting me whenever I needed help. I would like to thank Dr. Robert Horton for sharing all his wisdom and support generously.

I would like to acknowledge and thank my research group members Sajjad Satvati, Masrur Mahedi, and Yijun Wu for their support and help in the field. I would like to thank my METU family: Gizem Can, Makbule Ilgac and Dr. Kemal Onder Cetin for their unconditional support throughout this time.

I would also like to thank my dear friends Yuderka Trinidad, Conglin Chen, Yang Zhang and Paul Ledtje for making the office life full of joy and laughter. My dear Ames family: Guliz Tokadli, Tugce Karakulak Uz, Metin Uz, and Cem Kolbakir; I am so grateful to meet you! I am also very grateful for my best friends Oyku Han and Ahmet Emre Aydin, thank you for supporting me unconditionally, making me laugh and sending your love. I would like to thank Haluk Sinan Coban for everything you did, I am so lucky to have a friend like you! I am very grateful for having this precious family in Ankara, Turkey; Ertugrul Genc, Sevgi Atay, Songul Atay, Necip Atay, Kaya Can Atay and Doga Kayra Atay.

Most of all, the biggest thanks to my one and only mom for her support in every possible way, I cannot tell how grateful I am to have the best mom in the whole universe!

ABSTRACT

Granular-surfaced roadways, one of the most significant public road systems in the U.S., are highly vulnerable to be severely affected by the seasonal freeze-thaw cycles in cold regions. The state of Iowa is located in a cold region and experiences severe winter weather each year. To minimize the damage, seasonal load restrictions (SLRs) are applied, for typically 8 to 9 weeks from February to May. In addition, the Road Weather Information System is used to monitor the winter weather conditions, which consists of equipment to collect and transfer observations from roads. To help local transportation agencies with the organization of SLRs and resource planning, the development of a prediction model for different soil conditions around the state would be very useful. A great deal of cost savings could be achieved with a prediction model that captures the characteristics of the freeze-thaw cycles well and is updated with real-time weather and soil data. To develop such a model, an appropriate sensor network and data acquisition system must be planned and installed rigorously. In this study, the development and installation of the monitoring system are described, which is located in Hamilton County in central Iowa. The system consists of a weather station to collect atmospheric information and 80 sensors to measure soil water content, matric potential, and soil temperature properties from the subgrade of the roadway. This thesis presents the preparations that were done beforehand, installation procedures, and various post-installation problems and troubleshooting measures. The suitable sensors and data acquisition system were selected and coordinated to ensure successful installation and operation. Furthermore, laboratory and field trials were performed to minimize any installation or connection problems. This study also includes further details such as soil-specific calibration and grounding practices

as well as a preliminary discussion about the obtained field data. A brief comparison between the weather station data and measurements of the nearest active RWIS stations was made to determine whether the RWIS stations could replace the weather stations for future application of the prediction models in other locations.

CHAPTER 1. INTRODUCTION

Freeze-Thaw Cycles under Granular-Surfaced Roadways

In the State of Iowa, granular-surfaced roadways comprise one of the main public roads systems, along with interstate and local highways. These roads generally provide access to rural farmland, livestock production, and recreation (Iowa County Engineers Association 2019). They have both social and economic values in the region since they connect people in rural residency to jobs and schools, and facilitate seed and fertilizer distributions from suppliers. Granular roads are mostly preferred by Counties and the Department of Transportation (DOT) for secondary roads, because of their lower construction and maintenance costs compared to paved roadways.

Seasonal freeze-thaw cycles and the damage that occurs due to these cycles are the most significant elements affecting road conditions in northern cold-climate road networks in North America, Europe and Asia (Saarenketo and Aho 2005) (Figure 1). In cold regions, soil mechanical properties are significantly altered due to the effects of freezing and thawing on the soil's microstructure. Ice bonding between the soil particles during freezing and excess moisture gain during thawing decrease the bearing capacity of soils significantly (Konrad 1989; Wang et al. 2007).

To understand the freeze-thaw mechanisms in the soil, the basic laws governing the physics of soil, heat, and water transfer should be considered. In thermodynamics, the equilibrium state of the system should be satisfied by eliminating temperature-gradient; otherwise, heat transfer will occur in the system (Incropera et al. 2007). Therefore, the heat transfer phenomena of soil freezing would start with the temperature-gradient with depth. Meanwhile, the water content and its movement are altered by the temperature-gradient

increase. Due to this increase in the temperature-gradient for the case of frozen soils, the frost front penetration rate is high, and a suction gradient develops between the frozen and the unfrozen zones (Konrad and Morgenstern 1980). Consequently, water migrates from the unfrozen zone to the frozen zone as in liquid and vapor forms (Konrad and Morgenstern 1980; Zhang et al. 2016). The fast-advancing frost front freezes some of the migrated water surrounding the soil particles to establish an equilibrium, but is not enough to maintain a continuous ice lens at that level. Therefore, segregational freezing will occur on the surface of soil particles. However, as the rate of the frost-front penetrations decreases, the rate of temperature change across the soil is reduced, and this can produce discrete ice lens formations until the temperature gradient disappears. The formation of ice also alters soil stresses due to the expansion of water in the soil pores, and this pressure is relieved by heaving soil in the direction of least resistance (Konrad 1989). These effects can be amplified by greater increases in temperature gradient and water content in the soil. Therefore, much research has been focused on heat and water transfer aspects of soil freeze-thaw problems and the study of models that incorporate these coupled phenomena.

Coupled heat and water models have been studied in unsaturated soils for several decades. Early work of Philip and De Vries (1957) established a non-isothermal flow model with a relationship between volumetric water content and temperature gradients. Sophocleous (1979) modified that model using a matric head-based approach instead of volumetric water content, to preserve continuity between unsaturated and saturated layers, and Milly (1982) later included hysteresis into the model. Subsequently, Nassar and Horton (1992) incorporated osmotic effects into the model, and researchers have continued to develop further models to enable more accurate results. Freeze-thaw cycles have been investigated in previous studies

using these coupled heat and water transfer models (Cheng et al. 2014; Heitman et al. 2008; Kang et al. 2013; Milly 1980; Nassar and Horton 1997).

The size of the damage that can occur due to freeze-thaw cycles is mainly dependent on soil properties such as grain size distribution, plasticity index, moisture content; rate of freezing, and other environmental factors such as the availability of water and applied loads (Konrad and Morgenstern 1980). The damage can be kept at a minimum if these applied loads can be controlled. Consequently, temporary or permanent weight restrictions are applied in some seasonally cold regions such as Scandinavia, Scotland, Canada and the Northern U.S. to minimize the damage caused by freeze-thaw cycles (Orr et al. 2017; Saarenketo and Aho 2005). In the U.S., such restrictions are generally referred to as spring load restrictions (SLR) or seasonal load limits (SLL), and they are typically applied between late February or early March until the end of April or May, covering a period of 8 to 9 weeks. These restrictions may vary from state-to-state depending on the local government. For Iowa, SLRs typically begin March 1st and continue until May 1st (Ovik et al. 2000).

Figure 1.1 Damaged granular-surfaced roadway due to freeze-thaw cycles in Hamilton County, Iowa.

Other than applying the simple length-of-time technique with specified recovery periods for certain road types, there are three main resources for SLR placement and removal;

(1) Sub-surface instrumentation, (2) In-situ stiffness testing, and (3) Modeling (Orr et al. 2017). Sub-surface instrumentation or field monitoring is a site-specific application and generally done for soil moisture and temperature observations to capture sudden changes at the data during freezing/thawing. It can be considered as the most accurate method for freeze-thaw observations since it provides real-time, continuous in-situ measurements that enable secondary roads agencies to take action more rapidly. In-situ stiffness testing uses correlations to falling-weight deflectometer (FWD) and light-weight deflectometer (LWD) test results at certain points on a roadway and requires periodic field trips. Finally, modeling is the numerical calculation for SLR placements based on daily air temperatures or any other input (such as road surface and subgrade material properties, and/or atmospheric data) depending on the numerical model. These resources can be used separately or together for SLR placement and removal applications.

Field Monitoring

Soil is an extremely diverse material that requires specific classifications and different analytical treatments for different types. This is because it can possess large temporal and spatial variability and a strong dependence on weather conditions (Körschens 2006). Therefore, field experiments are very valuable in soil-related and geotechnical projects since they will be heavily influenced by such factors.

To investigate freeze-thaw cycles continuously in the field, various monitoring and analysis studies have been performed in the past. The Europe-based Roadex II Project focused on the Scandinavia and Scotland region to collect information about spring thaw weakening (Saarenketo and Aho 2005). The authors monitored the soil dielectric constant, electrical conductivity and temperature of two paved and three unpaved roadways in Scotland, Sweden, and Norway by installing percostations. They also conducted Ground Penetrating Radar (GPR)

tests to track the thickness of the structural layers. Another example is from Breton in Alberta, Canada. Soil moisture and temperature sensors were installed up to 100 cm deep, along with a weather station for meteorological data collection and an observation well for groundwater level monitoring (He et al. 2015). Overduin et al. (2006) used a transient heat pulse probe in Brooks Range, Alaska at a depth of 0.37 m where the groundwater table was located at 0.20 m depth. The sensor consisted of a thin film that includes heating wires. The study aimed to investigate the relation between freeze-thaw processes and the soil thermal properties. Finally, soil liquid water content and temperature were measured in northeast China down to a depth of 0.35 m (Cheng et al. 2014). The objective of the study was to compare results of a coupled heat-water transfer model to field measurements under freeze-thaw conditions.

Each of these monitoring systems was designed differently, but all were deployed at relatively shallow depths compared to those used in the present study. Additionally, they all involved field installation of custom sensor systems rather than making use of existing monitoring networks. In the U.S., some researchers have made use of existing networks of sensors stations and their data. One of the most common such monitoring systems present in the U.S. is the Road Weather Information System (RWIS).

Road Weather Information System (RWIS) and Its Stations

Transportation Agencies, especially in cold regions, typically employ field-monitoring systems to observe winter weather conditions for safety, maintenance, and operations. The Road Weather Information System (RWIS) is a fully-developed network consisting of hardware, software and communication interfaces that collects and transfers observations from roadways (Ewan and Al-Kaisy 2017; Manfredi et al. 2005) Figure 1.2 shows the locations of RWIS stations in Iowa. The data collection is achieved by Environmental Sensor Stations (ESS) consisting of sensors and equipment to monitor atmospheric, pavement, soil and water

level conditions (Manfredi et al. 2008) (Figure 1.3). These stations can be assembled to be mobile or stationary. Standard ESS include air temperature, relative humidity, wind speed, precipitation, surface and subsurface temperature sensors (Parsons Brinckerhoff and Iteris 2013). Some of the optional sensors are visibility, snow depth, and solar radiation sensors. These stations can be also constructed as partial units without some of the standard sensors depending on the budget or observation requirements. However, to provide consistency between different stations and present a general standardization, some guidelines are published regarding these ESS (Manfredi et al. 2005, 2008).

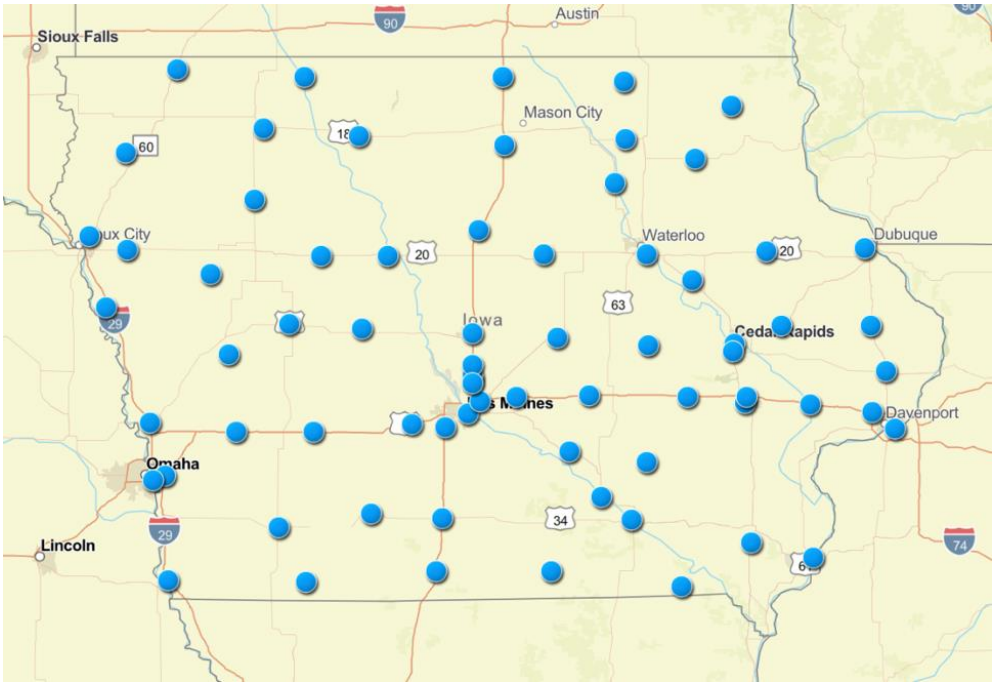

Figure 1.2 RWIS Stations in Iowa (taken from weatherview.iowadot.gov).

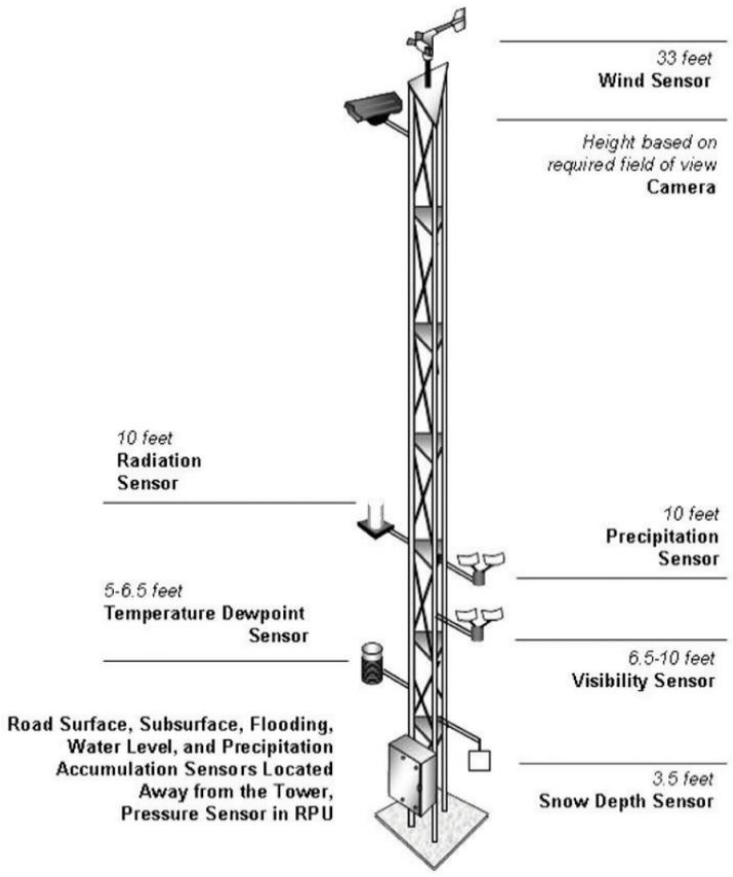

Figure 1.3 Typical standard ESS configuration (Manfredi et al. 2008).

The RWIS is used for pavement condition and weather forecasting in addition to real-time data collection. For forecasting, the enhanced integrated climate model (EICM) is typically used. The EICM is a one-dimensional heat and moisture flow model that merges atmospheric information such as rainfall, percentage of sunshine, cloud cover, wind speed and air temperature (Vavrik et al. 2016). This model is the most advanced version of pavement climatic modeling, which started as a heat transfer model in 1969 at the University of Illinois-Urbana Champaign (Beckemeyer 2015). Currently, it requires the following five fundamental climatic data inputs to perform several calculations: (1) air temperature, (2) precipitation, (3) wind speed, (4) percent sunshine, and (5) relative humidity (Zapata and Houston 2008).

Recent studies have shown that the weather conditions at un-instrumented, "virtual" observation sites could be extrapolated from instrumented locations using these forecast models, which is called virtual RWIS, or vRWIS (Parsons Brinckerhoff and Iteris 2013). These new developments may change the traditional winter maintenance and operation practices dramatically for transportation agencies. According to a survey of DOTs from 24 states, the responses showed that currently, 36% of DOTs spared low levels of their funding or effort on RWIS, with 60% sparing no funding or effort at all. However, in five years 35% of these DOTs speculated to spend 1-10% of their funding or effort on RWIS and 45% projected that the funding level would be more than 10% (Ewan and Al-Kaisy 2017). These results are also a clear sign for researchers to pay more attention to the RWIS data and its resources for addressing freeze-thaw problems and weather-related forecasting in the future.

Project Overview: Frost Depth Monitoring and Prediction

Winter maintenance and operations are essential to maintain the quality of the granular-surfaced roadways in Iowa. To support Iowa DOT and County Engineers on their work to arrange load restriction applications and the resource planning, a freeze-thaw prediction model for different soil conditions around Iowa would be useful. For this purpose, four granular roadway sections are proposed to be instrumented with soil moisture, soil temperature and weather station sensor systems (Figure 1.4). These measurements would be used to develop a frost depth prediction model and freeze-thaw forecasting tool for winter seasons.

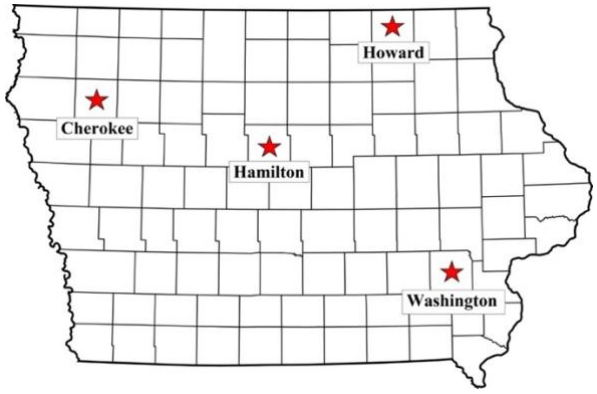

Figure 1.4 Four granular roadway section locations selected for the project.

Locations of the sites are selected to be representative for the various soil conditions present in Iowa. One of these four sections, the Hamilton County site, can be considered as the hub and the most advanced monitoring site in the project. It is located in central Iowa and it consists of 80 sensors in five boreholes throughout the road's cross-section. Boreholes are located at the center, shoulders and mid-sides of the roadway (Figure 1.5). Sensors were located every 30 cm (1 ft) up to a depth of 213 cm (7 ft) below the subgrade surface, with an additional sensor installed at 15 cm (6 in.) depth (Figure 1.6). The site also includes a weather station to collect climate data similar to the ESS. Therefore, atmospheric data will be available to compare with the nearest active RWIS stations, to study how their data can be interpolated to represent an "un-instrumented" site similar to the vRWIS system, to apply the freeze-thaw prediction model to other locations.

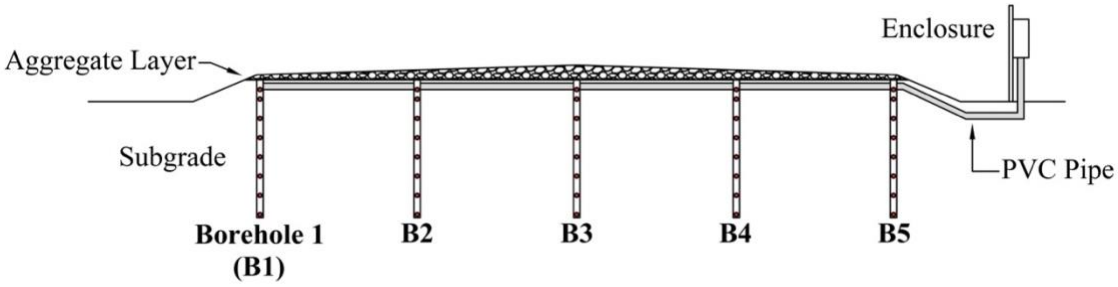

Figure 1.5 Cross-sectional view of the Hamilton County site.

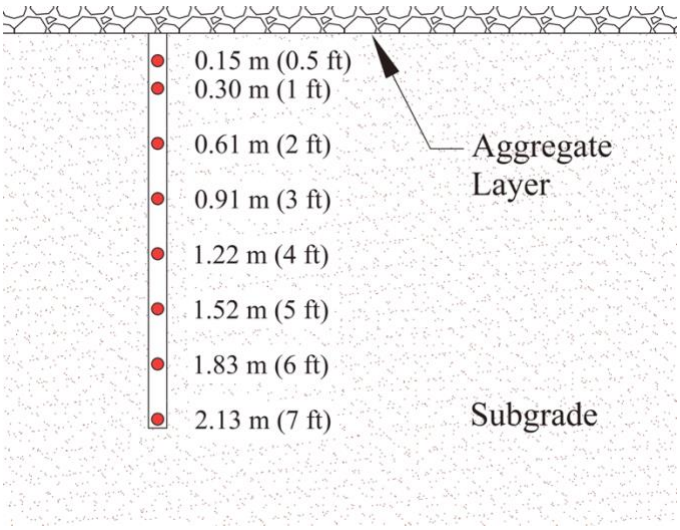

Figure 1.6 Sensor locations in each borehole

Three other sites were instrumented in Cherokee, Howard and Washington Counties, to obtain data from the north-west, north-east, and south-east regions of Iowa. These three sites were instrumented in a simpler way, but with only one borehole at the center and one at a shoulder, with the same sensor depths as shown in Figure 1.6. However, these three sites do not include weather stations.

Due to its complexity, sensor-richness and proximity to the university campus, the Hamilton County site was selected as the first field site to be instrumented. It is closely scrutinized in the present study with regard to the steps taken in the instrumentation and installation procedures.

Organization of the Thesis

This thesis is aimed to be a guiding resource to the future researchers for their installation preparations and applications. Chapters are organized according to the order of the instrumentation procedure as (1) Instrumentation, (2) Installation, and (3) Data Collection and Results.

The Instrumentation chapter starts from the steps followed to decide on the parameters to be collected, and continues with the identification and selection of convenient sensors for this specific study. It also includes some practical and helpful approaches for equipment selection and calibration. The Installation chapter focuses on the essential preparations required prior to construct the system in the field and the procedures to be followed during installation. The Data Analyses and Results chapter presents preliminary data processing, organization, and interpretation. The expected and unexpected developments in the available data are discussed with their possible explanations.

CHAPTER 2. INSTRUMENTATION

Choice of the Parameters

Rather than the conventional fieldwork procedure, the instrumentation actually starts by selecting the parameters to be monitored for a specific problem. The selected parameters that can be based on mechanical, hydraulic or thermal properties, should be sufficient enough to validate the research hypothesis and efficient enough to avoid requiring other sensors, which will eventually cost more. Since the purpose of this project is to investigate freeze-thaw characteristics and freezing/thawing fronts, there are two major concepts to consider: thermal conditions and hydraulic movement. Thermal conditions of the soil can be identified by observing the temperature change with weather conditions. In addition, a more sophisticated study can be conducted via taking heat transfer characterization into account during analyses. These terms include thermal diffusivity or volumetric heat capacity measurements (Heitman et al. 2017; Peng et al. 2017). However, this is not within the scope of this MS thesis.

Moisture presence in the soil media is an important parameter that needs to be considered for investigating the freeze-thaw behavior of soils. Hydraulic movement occurs not only due to the presence or absence of water in the medium, which is quantified as water content, but also its energy state. The energy state describes the effects of the surrounding's forces on the soil water and determines whether the water is able to flow or not in a particular direction (Jury and Horton 2004). Considering water movement in soils is relatively slow, the kinetic energy of this movement may be neglected during the calculation of energy state in the medium. Therefore, the state of the soil water is identified in terms of its free energy per unit mass, which is called total soil water potential. Soil water potential may consist of various components depending on the chemical and pressure conditions; however, "the matric

potential manifests the tenacity with which soil water is held by the soil matrix" (Hillel 2004). This means that matric potential is the most significant component of the soil water potential to capture the behavior. Matric potential and water content are correlated parameters, and the graphical representation of this relation is called soil-moisture characteristic curve (Hillel 2004). This relationship is not unique for a particular soil, and its feature depends on the wetting or drying history and changes in the soil structure (Hillel 2004; Jury and Horton 2004). Consequently, matric potential, temperature, and water content parameters should be used to be able to solve the phase change problem of water for freeze-thaw conditions in soils (Spaans and Baker 1996; Sun et al. 2012). Therefore, these three parameters are selected to use to get realistic results on freeze-thaw monitoring of the subgrade soil. After determining these parameters, a search is started to find the most convenient sensors available in the market to measure these parameters with accuracy.

Selection of the Sensors

Some essential properties need to be satisfied by the sensors due to the structure of the project and endurance related aspects. First of all, they need to be robust enough to survive in a borehole under the applied stresses by the traffic load. Secondly, the ranges of the different sensors vary quite a lot since they may have developed for different purposes, so the sensors should have appropriate ranges of measurement for this project. Furthermore, they should have adequate sensitivity to record slight changes in the medium.

There are various brands and models of water content sensors commercially available with different indirect measurement methods such as dielectric measurement, neutron scattering technique, resistivity measurement, and soil thermal property measurement. (Bittelli 2011; Huisman et al. 2003; Jury and Horton 2004; Mittelbach et al. 2012; Xu et al. 2011). Some of these methods are found unsuitable for this project because they either require further

calibration, it has more laborious installation procedure, or they are hazardous (Bittelli 2011; Topp et al. 1980). Therefore, the dielectric measurement method was investigated first since it seems to be easier to manage. In general, this method uses the differences in the intrinsic material property of dielectric constant (κ) between the soil phases to estimate water content in the soil medium, where water ($\kappa_{water} \approx 80$) has a relatively higher value than air ($\kappa_{air} \approx 1$) and solids ($\kappa_{solid} \approx 4$ to 16) (Bittelli 2011; Hallikainen et al. 1985; Topp 2003; Xu et al. 2011). In addition, the dielectric property is independent of soil's density, texture, and salt content and has no significant dependence on temperature (Topp et al. 1980). One of the examples for dielectric methods is Ground Penetrating Radar (GPR). It is an electromagnetic method which uses high relative permittivity (dielectric constant) for the water in the soil, which makes it practical to measure water content. It can be conducted in several ways. For instance, GPR transmitter and receiver can stay on the ground surface, and the reflections or the scatters from the interfaces or localized objects are recorded as the transmitter and the receiver move over the surface. The velocity of the signal would be the primary information used for predicting water content. Another application of this method can be placing transmitter or receiver or both into the ground, usually in access tubes, to measure the velocity of the signal from one to another (Topp 2003). There are some further applications available for GPR method; however, as it can be seen from these two examples provided, it is more suitable for the measurements on the broader/wider areas, continuous throughout the depth, but it would provide intermittent data which makes it unsuitable for this project (Topp 2003).

Another example of the water content measurement methods is the prominent Time Domain Reflectometry (TDR) (Ferré and Topp 2000). This instrument consists of a step generator, a sampling receiver, and an oscilloscope (Baker et al. 1982). Step generator (prong

with two parallel arms to form waveguides into the soil) sends a step pulse of electromagnetic radiation along with the guides, and at the end of the prong, this pulse is reflected and returned to the source. This radiation signals' travel time and velocity are estimated with the oscilloscope, which is then used to predict the dielectric permittivity property of the soil. TDR is a known method for its accuracy with a wide range of soils without soil-specific calibration requirement. It is also relatively easy to use, providing real-time fast in-situ monitoring, and available for automated remote monitoring with the usage of datalogger and multiplexers (Topp et al. 2008).

Similar to the TDR Method, capacitance and frequency domain sensors also work to estimate dielectric permittivity in soils. Capacitance sensors also have prongs that can send electromagnetic waves back and forth in a direction, but they measure the capacitance of the medium differently. On the other hand, frequency domain sensors measure dielectric properties of the reflected electromagnetic wave in the frequency domain in order to obtain dielectric properties of the medium (Bittelli 2011). The combined version of these sensors that includes both frequency-domain reflectometer and capacitance sensors are called dielectric sensors or electromagnetic sensors (Bittelli 2011; Robinson et al. 2003). These methods are mainly preferred since they are relatively inexpensive, adaptable, easy to operate and less destructive to the soil structure (Kelleners et al. 2005; Robinson et al. 2003; Sun et al. 2012; Topp 2003; Xu et al. 2011).

The commercially available options were observed and checked from various vendors. The main differences between the sensors besides the methods they are using are their measurement ranges, prong length and diameters, and prices. In a previous study, the capacitance sensors have been found inadequate due to its limited VWC measurement range

and low sensitivity (Mittelbach et al. 2012). Prong length is also a significant issue for the sensors. For instance, it is more representative with longer needles, but they are more difficult to install without bending the needles (Mittelbach et al. 2012; Xu et al. 2011). Considering the more overall robust structure for the granular-surfaced road conditions and wider range of VWC measurements, a dielectric sensor named "GS1" which uses capacitance and frequency domain technology, from Meter Environment (formerly Decagon Devices) is selected to monitor the soil water content during the project (Decagon Devices 2015a) (Figure 2.1(a)).

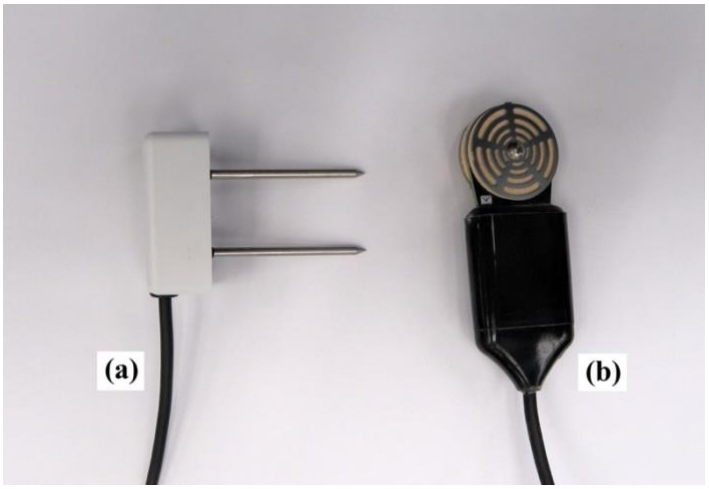

Figure 2.1 Selected sensors for the project: (a) GS1 for soil water content measurement and (b) MPS6 for both soil temperature and matric potential measurements

For the in-situ matric potential measurements, the alternatives are not as many as water content sensors. In general, the soil matric potential measurements are based on three methods: (1) solid equilibrium methods, (2) liquid equilibrium methods, and (3) vapor equilibrium methods (Cobos 2019). Even though each of these methods uses different materials, all of them are based on the equilibrium of the material matrix to the soil water conditions. Then, they take the measurements accordingly.

For the field applications, tensiometer is one of the main matric potential measurement tools that is preferred due to its high accuracy. The design of tensiometers is based on the liquid

equilibrium method. Thus, it equilibrates water in tension to the soil water through the porous cup (Cassel and Klute 1986; Cobos 2019). However, its typical matric potential range is 0 to -100 kPa, which could limit the measurements under frozen and very dry condition. Moreover, this instrument cannot be connected directly to a digital system (Cassel and Klute 1986). There are some digital tensiometers which can be connected to a datalogger to obtain continuous measurements at deeper points in soils. However, the application depth is limited for the commercially available tensiometers in the U.S., and they cannot provide digital data for constant data reading. Due to these reasons mentioned above, solid equilibrium methods such as electrical resistance or capacitance sensors become more suitable due to their ability to connect to dataloggers for constant measurements. In addition, the cable lengths of these sensors can be adjustable depending on the planned depth for monitoring. There are available products in the market that work with this method. However, they have various measurement ranges and accuracy levels. After a thorough investigation, MPS6 model of water potential sensor from Meter Environment is selected to be used in this project (Figure 2.1(b)). This sensor uses a ceramic disc to be equilibrated with the soil water, but it uses dielectric permittivity of the disc to calculate water potential at the medium (Decagon Devices 2015). Besides, this device includes a temperature sensor inside that can provide two measurements digitally and simultaneously.

These two selected sensors have the option to be custom-made according to the required cable length for deeper measurements as applied in this project. The corresponding cable lengths were calculated by taking the dimension of the road width, foreslope and ditch length from the field. The enclosure that the cables should eventually reach is decided to be put close to the backslope to provide some clear spacing from the road and to be able to

maintain accessibility even after snow events. Extra of three feet was added for each sensor in case of any shortage that can be encountered during the installation process. The issues faced due to this calculation is further discussed in the "Recommendations" section.

For the weather station selection, the most crucial criterion is the compatibility of the system with the Road Weather Information System (RWIS) stations in Iowa. It was important to evaluate whether the selected weather station is suitable for interpolating nearby RWIS stations data for inputs to the prediction models versus using local roadside weather data. RWIS can be considered as one of the major weather data sources for the transportation community (Ewan and Al-Kaisy 2017). It consists of advanced sensors for the collection of atmospheric, pavement, soil, traffic, environmental, and hydrological information (Kwon et al. 2015; Parsons Brinckerhoff and Iteris 2013). The main purpose of the system is to support DOT personnel for winter maintenance applications and in case of any additional actions needed, traffic management strategies and pavement condition forecasting (Ewan and Al-Kaisy 2017; Kwon et al. 2015; Parsons Brinckerhoff and Iteris 2013). These stations typically consist of atmospheric sensors such as air temperature, wind, precipitation sensors; pavement sensors such as surface and subsurface temperature sensors; and camera imaging. Unlike the typical roads where RWIS is present, this project focuses on the freeze-thaw characteristics of granular-surfaced roadways. Therefore, some adjustments had to be made accordingly, by considering essential parameters required for EICM, and five main atmospheric sensor types were decided to be collected from the selected weather station: (1) precipitation, (2) wind speed and direction, (3) solar radiation, (4) air temperature, and (5) relative humidity.

There are various types of weather station systems available in the market. The vendors have packaged weather stations with a certain type of sensors included within the system, and

they usually do not allow external adds-on. This option can be more favorable for the applications where the time is the most critical factor that cannot be spared. There are modular types where the sensors can be exchanged or eliminated according to the measurement requirements within the vendor's convenience. This option can be convenient if the adequate sensors have been found in the limited list provided by the vendor. There are also commercially available sensors that can be ordered separately and combined manually by the researchers where data logger systems should also be considered independently. This method requires more time and effort than the others, and additionally these separate orders may end up with a more expensive instrument than what was intended. Finally, there are composite weather station systems that are compact unibody systems that do not require additional datalogger system or consistent with the existing multi-purpose data logger systems. This option is very similar to the packaged type; however, it would gain an advantage on the overall battery power usage and installation easiness compared to the composite options. After the evaluation of these types, their specifications and costs in the market, ATMOS 41 model of the composite weather station from Meter Environment was selected for this project (Figure 2.2). Later, the data collection interval was chosen as 10 minutes since it is the interval used for the RWIS stations in Iowa.

Figure 2.2 Selected weather station for the project, ATMOS 41.

Data Acquisition System

Data acquisition (DAQ) system is an essential component of the monitoring phase. After sensors are selected, there is a limited type of dataloggers left to be used that are compatible with all selected sensors. There were preconfigured dataloggers available from Meter Environment with limited connection ports for sensors, and there were general-purpose dataloggers that have multi-purpose structure, connection availability for a higher number of sensors (and can be augmented even higher with multiplexers) and high adaptability to various types of sensors. However, these dataloggers require further programming to define the measurement sequence, data storage, and power efficiency. By considering the prices, various sensor types to be used and past experiences with the equipment; CR1000X datalogger from Campbell Scientific is selected to be used for this project (Figure 2.3).

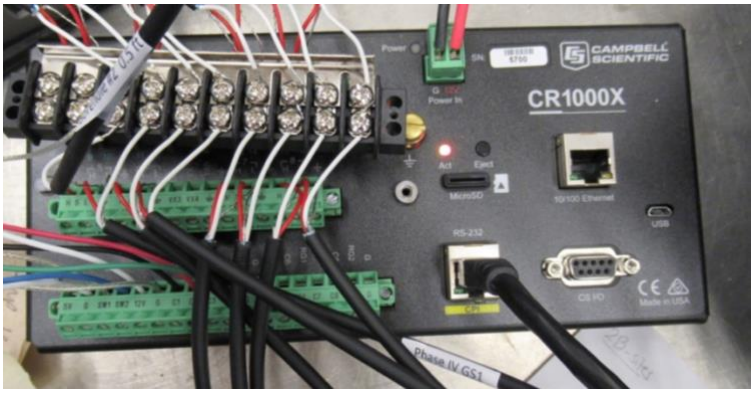

Figure 2.3 Selected datalogger for the project, CR1000X.

The AM16/32B multiplexer from the same company is selected to satisfy the need for a higher number of connected sensors (Figure 2.4). Each multiplexer has 32 groups of two lines that can handle the GS1 or MPS6 sensors. GS1 is an analog and MPS6 is a digital sensor which is important for the output signal obtained by the data acquisition system. The multiplexers could be programmed for either analog or digital output structures. Therefore, a total of three multiplexers were required for a system of 80 sensors that has 40 analog and 40 digital sensors. Two of these three multiplexers will be used for MPS6 sensors, whereas the other one will be used for GS1. There will also be eight available groups of two lines left for the rest of the GS1s at the datalogger.

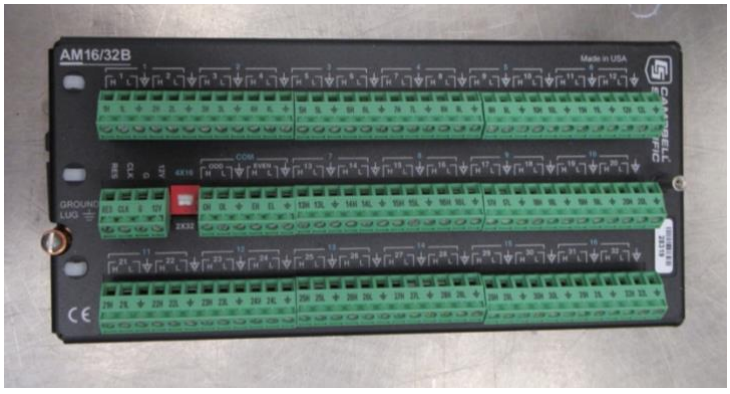

Figure 2.4 Selected multiplexer for the project, AM16/32B.

For three-wire interface analog sensors, there are two types of voltage measurements; (1) single-ended (SE) and (2) differential-ended (DE). Single-ended measurement provides the voltage difference between the data wire and ground wire, and it is the best option in case of the limited number of ports, but it sacrifices accuracy of the measurements. Differential-ended provides the voltage difference between two wires, which makes it independent from the ground reading and provide the ability to avoid noises by letting them cancel each other. So, DE measurement is decided to be used except for the ones connected directly to datalogger, because there is not enough port left to satisfy DE after multiplexer-datalogger connections would occupy some ports.

For digital sensors, the two most common types of communication considered are; (1) SDI-12 and (2) RS 232. For SDI-12, it is a communication protocol between the sensor and the data recorder that provides the serial-digital interface. It is advantageous when lower equipment cost is planned, minimal current drain is needed from the battery-powered system or single data recorder is available for multiple sensors through one cable. However, it becomes problematic for the systems that demand constant attention and not tolerant of occasional data loss (Decagon Devices 2015b; SDI-12 Support Group n.d., 2019). On the other hand, RS 232 is the simple conventional standard for data exchange that does not have the risk of data loss or complicated, inevitable technical problems. It only requires enough number of the port for direct connection with the system, that is why it would be used in this project for digital sensors.

In previous studies, the data was downloaded by going to the field and manual data transfers. Since the test sites of the project are distributed (Figure 1.4) around the state, this manual data transfers would be a waste of time and work. In order to avoid these problems and

organize remote connection directly with the dataloggers, RV50 wireless 4G cellular gateway (Figure 2.5) is included in the equipment. Its purpose is to upload or update programs, monitor the status and health of the equipment, provide data that is downloadable and ease the troubleshooting.

Figure 2.5 Selected cellular modem for the remote connectivity, RV50.

Battery and Solar Panel Calculation

The proposed monitoring system for this project requires to survive at least two years without external support. A system like that should have enough battery power and enough size of the recharging element, the solar panel. These could have been calculated by considering the wiring configurations, power requirements of the sensors, and other elements. The weather conditions also play a significant role in the recharging since cloudy sky or less available daylight may delay the process. All of these factors are reflected in the power usage calculations in Campbell Scientific's "Power Budget Spreadsheet", which is also used in this project (Albers 2017; Campbell Scientific 2014) (Figure 2.6). Fortunately, Campbell Scientific's equipment has already been defined in terms of their power requirement, but sensors and weather station from another vendor needed to be defined manually. After entering the location of the system to calculate solar input, the battery and solar panel size are evaluated

automatically. According to the obtained results from that spreadsheet, a 24 Ampere-hour 12 Volt battery, and a 20 Watt solar panel were included in the 80-sensor monitoring system for Hamilton (Figure 2.7).

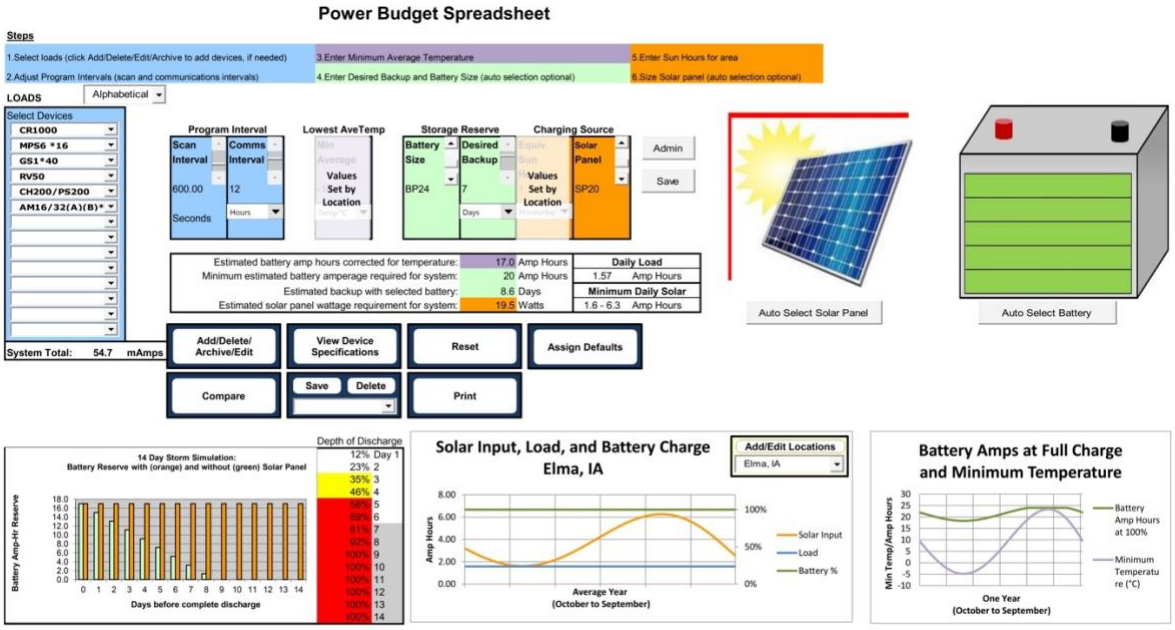

Figure 2.6 Screen capture of Power Budget Spreadsheet calculations for 80-sensor network (Campbell Scientific 2014).

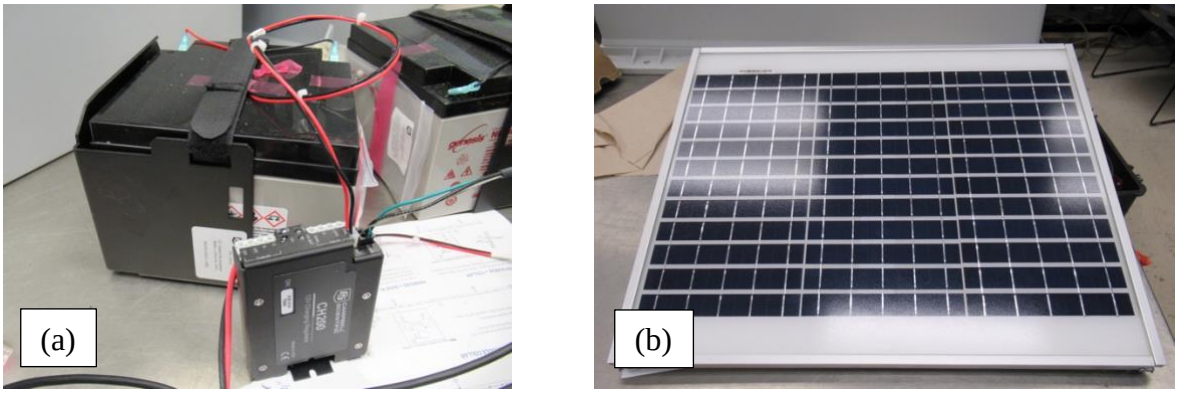

Figure 2.7 Equipment selected according to the Power Budget Spreadsheet results: (a) 24-Ampere hour 12-Volt battery, BP24 and its regulator, CH200; (b) 20-Watt solar panel, SP20.

Sensor Calibration

Calibration is important to avoid or reduce sensor bias in the measurements (Evett et al. 2006). For the selected water content sensor, the general equation provided by the vendor offers the foundation to compare soils and obtained by the factory calibration to cover a wide range of soils; however, it may provide slightly different values than the actual measurements such as overestimated values for oven-dry samples (Seyfried and Murdock 2004). Therefore, soil specific calibration is needed for collecting accurate readings.

The general equation provided in the manual of the sensor correlates raw millivolt output (mV) to volumetric water content (VWC) in the medium as follows (Decagon Devices 2015a):

$$\theta = 4.94 \times 10^{-4} \times mV - 0.554 \qquad (1)$$

Meter Environment, the vendor of the sensors, suggests this equation to be used for the majority of mineral soils since the GS1 sensor is insensitive to variations in texture and electrical conductivity due to its high measurement frequency, yet still encourages to perform soil specific calibration for the measurements where higher accuracy is demanded or required (Decagon Devices 2015a).

The provided soil-specific calibration method A is the recommended method that explains the formation of the calibration function step-by-step to be used on the sensors. It aims to take mV measurements with the sensor at various water content values where the actual water content is determined using the direct oven-drying method in the laboratory. An important point to consider is that the soil sample should be compacted to the estimated bulk density in the field. This would avoid the air gaps that may affect the calibration. The mV values from the sensors and the water content results from the direct method are plotted against

each other to form the calibration curve (Figure 2.8). The curve equation determined by linear regression method would be used as the soil-specific calibration equation for that location. This procedure is applied on a soil taken from the subgrade of the Hamilton site to obtain the soil-specific calibration curve.

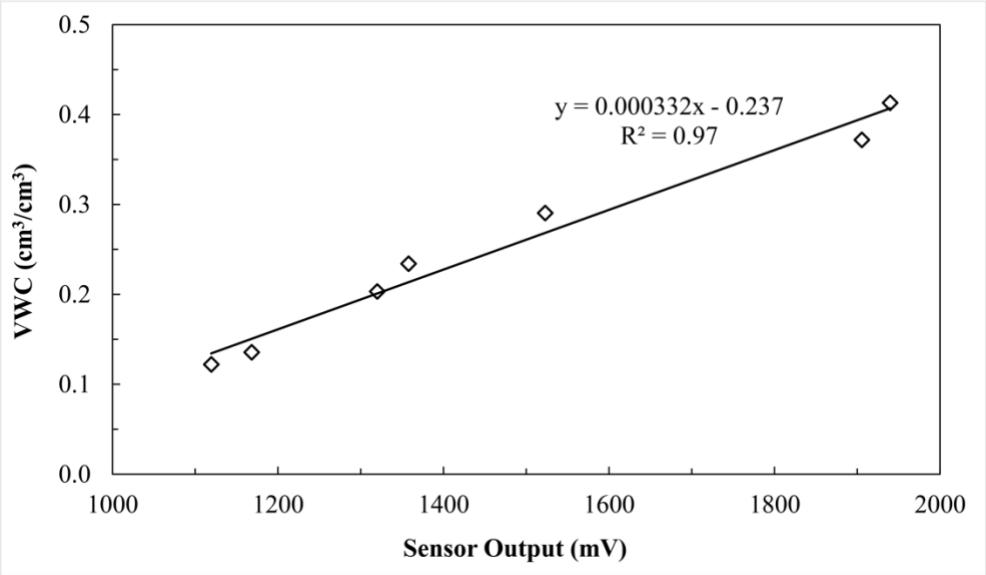

Figure 2.8 Soil-specific calibration for Hamilton County subgrade GS1 sensors.

CHAPTER 3. INSTALLATION

Preparations Before the Installation

After the sensors and the data acquisition (DAQ) system have been determined and ordered, the next step was to start planning for the installation procedure in Hamilton County. As it is shown previously, this application covers five columns of embedded sensors up to 2.13 m (7 ft) depth each. Therefore, an effective and practical installation methodology should be selected for this 5-borehole, 80-sensor system.

Furthermore, these two sensors have their suggested installation procedure provided in their manuals, and the plan should be coherent with that, as well. For instance, GS1 sensor is recommended to be installed into the undisturbed soil face of an excavated borehole. It should be inserted there and pushed completely until the electric cable is straight. Although it has sharpened-edge prongs to ease the installation, the prongs may be bent if the procedure would not be completed correctly (Liu et al. 2013). MPS6 sensor, on the other hand, is not affected by the air gaps or soil disturbance, but instead, the good hydraulic connection is essential for it as it will equilibrate to its surroundings. Its recommended installation procedure is to take wet native soil and pack it in a ball around the sensor, which should ensure moist soil contact with the ceramic disc.

For a fast solution, the sensors could have been aligned inside a PVC pipe which is filled with foam or any other filling material to avoid anything to pass through it and pushed into the soil. However, this solution does not ensure the required contact between the sensors and the subgrade. Besides, the sensors are not small enough to make this method efficient. Another considered method was to dig a trench throughout the roadway section and insert the sensors by hand or a simple tool that can go deeper into the soil. Nevertheless, it would have

caused a high level of disturbance in the soil which is not preferred. It is also not efficient in terms of time and budget. In addition, digging a trench that goes 2.13 m (7 ft) deep or even its half-way is not considered as a feasible work. Finally, the drilling borehole for each sensor column seemed to be the most practical option for this application because it would not cause a significant disturbance to the subgrade if it is compacted properly. Moreover, this method would still provide enough space for researchers to achieve an effective sensor installation.

To protect the sensor cables from the daily traffic in case of any revelation or against possible animal occupations and convey from the top of the boreholes through the enclosure, PVC conduit is planned to be used. There are more flexible options such as cable tubes or sleeves, but it is decided that those methods would not be as protective and effective as desired. The total length, diameter, type and number of fittings needed for the PVC conduit is calculated using the road width, foreslope and ditch distances, total number of cables passing and an area calculation for them, and lengths of the unibody PVC pipes that are sold in retail companies.

Another significant procedure is the arrangement of the preliminary programming plan. This includes the selection of the software to be used in datalogger, connection protocols to be used for high number the sensors and the actual connection diagrams to be followed after the installation. The software selection is important since the capability of programs may provide beneficial features such as manual programming to form the most efficient system or automatic data download commands. Considering the project's needs, program's features, and the budget opportunities, PC400 software is ordered from Campbell Scientific for CR1000X datalogger. It can support manual programming that is needed for various types of sensors and telecommunication options with the full-featured program editors (Campbell Scientific 2019a). The connection protocols that would be defined in the program have been determined as

previously discussed according to the concern levels in data safety and continuity, power efficiency, and port availability in datalogger or multiplexer. Additionally, wiring diagrams are generated, which is a valuable task for the program organization, first wiring and its checks, and in case of troubleshooting. It will be the only interface available after the installation so it should be simple and clear for any user. For this project, wiring diagrams are made as an AutoCAD drawing and a table.

Data acquisition equipment is one of the most vulnerable parts of the monitoring system with all its electronics and connection ports. Its safety should be ensured, to be able to continue short- or long-term data collection, with the usage of a high-quality enclosure with adequate robust and proofing properties. There are various sizes of weather-proof enclosures to contain these kinds of electronics on outdoors. By making a preliminary organization for all electronics and the cable lines location-wise, the required enclosure size could be calculated. In addition, it is always worth to order it with a few inches longer/wider/deeper or one bigger size of it since there could be some unexpected elements to be put. A larger enclosure also provides free space to work easier. For this site, a weather-proof enclosure with the size of 61x61x25 cm (24x24x10 inches) is selected according to a preliminary organization (Figure 3.1). The materials also vary for the enclosures, but the ordered case is made of fiberglass-reinforced polyester. This material is useful due to its light-weight, which is important for mounting easiness. It is also strong and leak-proof even after heavy winter conditions in Iowa during winter 2018-19.

Figure 3.1 Enclosure used in Hamilton site to protect DAQ equipment.

After the preliminary design of the enclosure, the electronics and the cables are organized in detail on the subpanel by using AutoCAD, since now the enclosure size is certainly known (Figure 3.2). Any need for additional supplements is checked such as wire ducts for more effective cable positioning or handles to carry the subpanel inside the case more easily. Last but not least, the mounting part for the solar panel and the weather station is designed. A 4.6 m 15 ft long steel round tube is used for this purpose. According to RWIS Guidelines, the majority of the weather stations should be 3 m (10 ft) or higher above the pavement surface. For granular-surfaced roadways, dust often occurs after each vehicle pass, which may cover the sensors of the weather station and cause reading errors. Therefore, the weather station is planned to attach at the top of the 4.6 m (15 ft) steel tube (Figure 3.3).

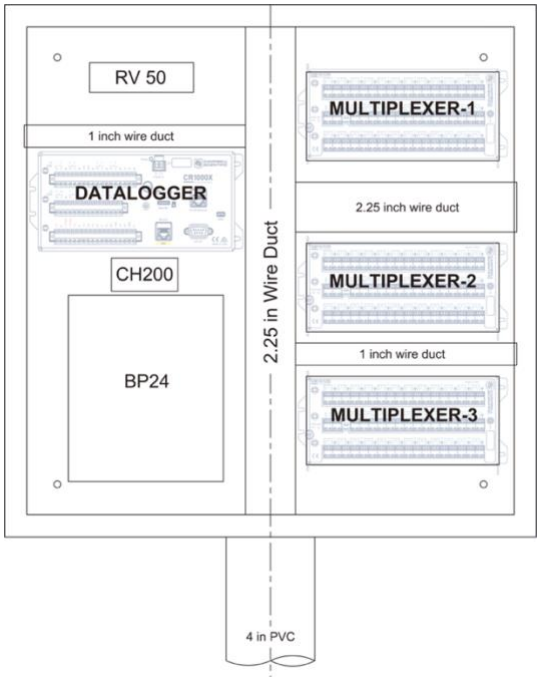

Figure 3.2 Layout of DAQ system in the enclosure.

Figure 3.3 Installation of the weather station at the top of the steel tube.

Final preparation before working in the field is the wiring practice in the laboratory (Figure 3.4). A big size desk is reserved for this procedure. The sensors are grouped by their boreholes on that desk and connected to the predefined ports in either datalogger or multiplexers. The purpose of this is to practice wiring before the actual sensor installation in the field. The sensors are also labeled near both ends with laser printable, self-laminating, ultraviolet (UV) and water-resistant adhesives according to their borehole and depth locations to avoid any confusion during field installation. Since the extra cable of the sensors may be cut after the installation, temporary labels from regular paper also produced and attached primarily at their tail.

Figure 3.4 Laboratory practice wiring.

Installation Tool

As the installation method for the sensors is determined as discussed before, the suggested installation procedures are checked for each sensor. As the properties of each sensor measure are different, the facts and conditions also change for the sensors that they are sensitive to. For instance, the MPS6 sensor requires a good hydraulic contact to achieve water

equilibrium between the medium and the ceramic disks, whereas it is not required for the GS1 sensor. GS1 measures the soil moisture between the two prongs, which makes it more sensitive to air gaps and soil disturbances. For the prongs to be emplaced into the borehole wall for various depths with a maximum of 2.13 m (7 ft), a pushing mechanism is needed. This can be provided with various type of methods, but there has not been any available tool in the market designed for this purpose yet, so the next step was to develop an installation tool for GS1 to be installed at 2.13 m (7 ft) depth in a borehole.

The required properties for the tool was a grabber and a pusher for the sensor. Some possible existing tools with similar mechanisms, which are built for different purposes, are checked. These tools include trash pickers or a simple lever arm. The trash pickers have arms that are generally much shorter than 2.13 m (7 ft). The arm can be elongated by building a new picker for this purpose only, but it required time and effort to build so other options are examined.

After some observation, a simple hold and release mechanism are developed with two different diameter PVC pipes interbedded. These two pipes have a little larger opening than the size of the sensor, so when the gaps overlap, the sensor is released and when the inner pipe is pulled, the size of the opening reduces, and the sensor is held in place. To avoid pipes to rotate, a screw and a bit are put at the top that is allowed to move in up-down direction only. A prototype is produced to see its practicality. A long wood board is used as a lever arm for pushing. Even, it satisfies the holding, the tool could not accomplish pushing the sensor in a smaller diameter of borehole, and it became very heavy to lower down in a borehole, so this option is abandoned.

Another prototype is produced by using the wood board with dimensions of 5x10x244 cm (2”x4”x8 ft), which is used as a lever arm before (Figure 3.5). A small pocket is routed at the lower end to place the sensor, and an adhesive putty is used to hold it in the pocket temporarily. Putty is not a very strong material so it can also enable the sensor to release once it is inserted in the borehole wall. For pushing, another type of mechanism is used this time. A simple wheelbarrow inner tube is attached at the back of the board with rubber bands to provide horizontal force for pushing the sensor into the soil. Its air valve is connected to a hand-operated pump at the surface of the borehole. To accomplish the installation, firstly the inner tube is planned to be deflated, and the negative pressure was locked in using a ball-valve to keep it flat as the board is inserted into the borehole. After the intended depth is reached for the sensor, the inner tube should be inflated until the prongs are pushed into the soil completely and then deflated again under vacuum pressure and the tool should be retrieved from the borehole to finish the procedure. This method was tested in Spangler Geotechnical Laboratory in Ames, Iowa. The borehole with 4-inch diameter was drilled with a hand auger and a sensor was installed at few different depths such as 0.3 m (1 ft) and 0.91 m (3 ft). The method succeeded in the trial testing, so it is planned to be used in the final installation. However, it could not be tested for the depths under the groundwater table which is a big challenge for the tool to hold the sensor, achieving the pushing and ensuring the successful installation after the tool retrieved.

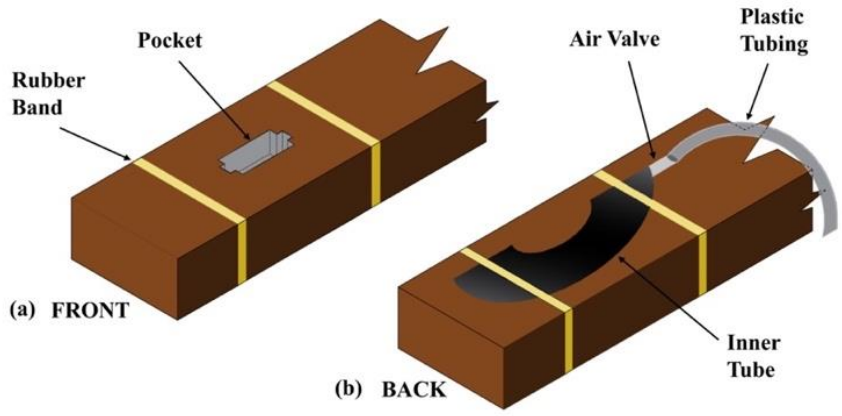

Figure 3.5 Prototype of the borehole installation tool developed for GS1: (a) front face, (b) back face.

While this prototype is being developed and tested, Meter Environment, the vendor of the sensors, launched a new borehole installation tool designed especially for their Teros type sensors that have a similar structure and dimensions to the GS1 sensor (Figure 3.6). It is a tool that has sophisticatedly designed with holding and pushing mechanism for the sensor. It pushes the sensor into the borehole wall when the handles are rotated in a vertical plane at the top. It also requires 10 cm (4-inch) diameter borehole particularly to lean the tool other side of the wall for pushing. However, the only limitation of this tool is that it cannot go deeper than 1.83 m (6 ft) depth without any additional work. This tool was rented for the field installation considering the possible problems that may occur with the developed installation tool.

Figure 3.6 Teros Borehole Installation Tool kit with an auger.

Field Testing Before Installation in Hamilton

A small-scale trial field testing is planned to check the practicality of the determined methods and functionality of sensors and the DAQ system. Instead of the whole system, only two of each type of borehole sensor are used in this testing with the weather station and the DAQ system. The monitoring system is planned to be checked outside of the laboratory conditions and near the university campus to provide quick intervention in case of a problem, so Beef Nutrition Farm on North Dakota Avenue is used as the testing field (Figure 3.7). Enclosure with the DAQ system attached to its subpanel and the weather station were mounted on an existing wood frame similar to what is planned for Hamilton County field. The sensors were installed at 0.30 and 0.61 m (1 and 2 ft) deep and the installation of GS1 is completed with the rented Teros Borehole Installation Tool. Then, the sensors were connected to the datalogger to start the testing. Remote connection to the datalogger with the cellular modem is also one of the significant checks that are aimed for this testing (Figure 3.7(c)). Other possible problems related to programming, power usage or wiring was also aimed to be detected if there was any and no problems were found after a week of monitoring. Therefore, the system was deemed ready for the final installation in Hamilton County granular road test site.

Figure 3.7 Beef Nutrition Farm: (a) general view of the site, (b) location, (c) testing point.

Final Installation at Hamilton County

After both laboratory and field testing were completed, the final and main installation at Hamilton County site was planned. The installation started on Thursday July 5th, 2018 and was completed without wiring the sensors on Friday July 6th, 2018.

The main heavy construction equipment was provided by the Hamilton County Engineer, which included a backhoe for trenching and skid-steer with 10 cm (4-inch) diameter auger mounted for the boreholes (Figure 3.8). The boreholes were placed throughout the cross-

section, so in order not to block the traffic on Vail Avenue, one-side of the road was kept open while the operation was started at the other side.

Figure 3.8 Heavy construction equipment used in Hamilton site installation: (a) backhoe for trenching, (b) skid-steer for the borehole drilling.

As the first step, the 10 cm (4-inch) thick gravel course was removed and a 15. 2 cm (6-inch) deep trench was dug below this gravel layer by the backhoe only for the half of the road. This 15. 2 cm (6-inch) trench is used for both the installation of the shallowest sensor depth and as a 5 cm (2-inch) cover for the buried 10 cm (4-inch) diameter PVC conduit that protects and transmits the sensor cables throughout the road section. Secondly, boreholes were drilled, and sensors were installed. The installation started from the furthest borehole from the enclosure (Borehole 1), and it was drilled with the auger of the skid-steer (Figure 3.9). For the backfilling and MPS6 installation purposes (explained previously in this chapter), native soil should be collected as much as possible. Therefore, cardboard with a 10 cm (4-inch) diameter hole in the middle was placed at the top of the surface to help capture the spoils from the borehole and the auger (Figure 3.10). This collected native soil was stored in the sealed buckets until they used for the aimed missions.

Figure 3.9 Drilling the first borehole with a skid-steer auger.

Figure 3.10 Cardboard placed at the surface to capture the spoils.

After the desired depth was reached for the borehole, sensor installation was started. The first sensor to be placed was GS1. The developed installation tool that tested in a drier and shallower depth was used at first (Figure 3.11). However, the installation was unsuccessful due to the high groundwater table around 1.22 m (4 ft) depth below the ground surface. This

prevented sensors to be hold in the pocket and inner tube to push the sensor into the wall. Fortunately, Teros Installation Tool was also brought to the site in case of any problem, and it was used without any need of an extension since 6-inches trench has been dug before. This second attempt with this industrially developed installation tool was successful, so it is used for the rest of the GS1 installations. The level is covered with a few inches of soil after GS1 was placed and then lightly compacted. Meanwhile, the circular ceramic disc of a MPS6 sensor was covered with the native soil that collected before from the corresponding depth and then lowered into the borehole until it reached the bottom (Figure 3.12). More soil is poured into the borehole to cover until the next desired installation depth has been reached. This process is repeated up to the top of the borehole. The first three boreholes were completed on the first day of installation, and the rest were completed on the second day.

Figure 3.11 Installation trial with the developed installation tool for GS1.

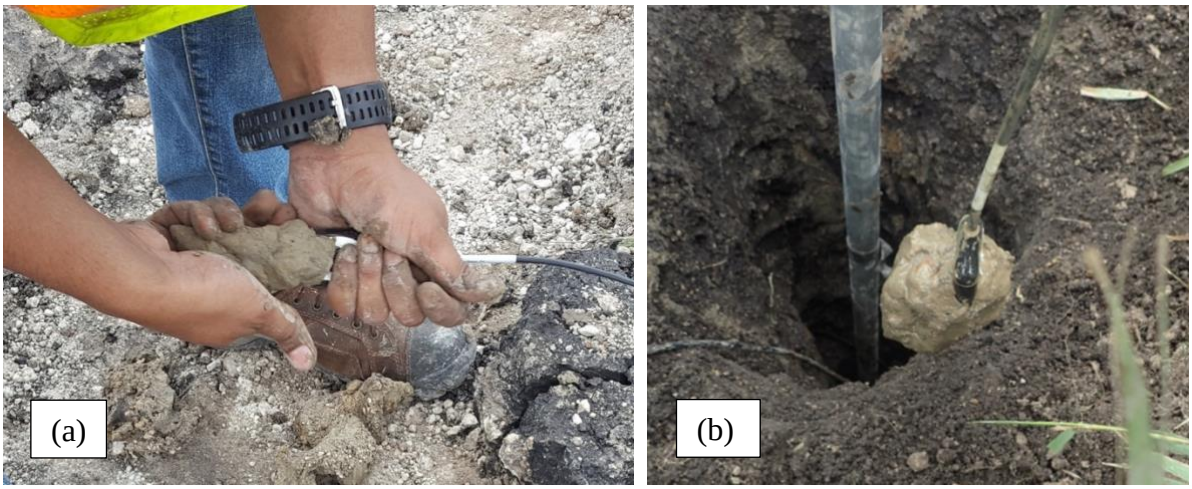

Figure 3.12 Installation of MPS6: (a) packing native soil around the ceramic discs of MPS6, (b) releasing the sensors down with the soil around.

For the MPS6 sensor, no recommendation is found regarding the installation orientation of the sensor to be horizontal or vertical in its manual. On the first three boreholes that have completed first, MPS6s were placed in horizontal position, and the last two boreholes the orientation was vertical for them. This configuration was used to determine whether the positioning would impact on the sensor measurements.

As sensors were placed to the planned depths, the cables were gathered at one side of the borehole wall with some slack left to ease backfilling and compacting. When the 15. 2 cm (6-inch) depth below the subgrade was reached for the last set of sensors, a small soil mound was built up over the backfilled borehole, and the last set of sensors were installed into that. The cables were collected for one last time to be pulled through the PVC conduit by using a fish tape (Figure 3.13).

Figure 3.13 Pulling the cables through fittings and PVC pipes at the bottom of the trench in subgrade.

Overall, there were some challenges and inevitable problems that were faced during the process, but the most significant one was the groundwater table. It made installation difficult below its level even with the Teros Installation Tool. It may have taken a few attempts to achieve the installation. In order to stop this problem, a simple water-bailing tool was formed from a stick and two plastic bottles (Figure 3.14). However, that did not perform well enough, so a 12-Volt water pump was used to discharge the groundwater filling the borehole (Figure 3.15). Nevertheless, groundwater filled the borehole faster than the discharge rate, so this method was not as effective as desired.

Figure 3.14 Simple water-bailing tool formed to discard excess water in boreholes.

Figure 3.15 12-Volt water pump used to discharge groundwater.

Last step before letting the sensors work was to route the cables to the enclosure, which had the DAQ system inside, through the PVC conduit and connected them to the corresponding ports that were planned before.

Grounding

The sensor system as assembled in this project, are made from delicate inner circuitry elements even though they may have built-in setup to protect against small-scale power surges. However, additional electrical grounding is very significant against larger-scale problems such as lightning surges and yet it could be easily ignored possibly to avoid additional works. The systems without these electrical grounding elements have the risk of intermittent problems or even complete system failures.

The datalogger and multiplexers have their individual grounding outlet embedded within their bodies that requires #14 AWG and #8 AWG wires to be connected to the earth via a ground rod, respectively (Campbell Scientific 2019b; c). For the sensors, the system can be planned by positioning ground rods at least 2 m (6.5 ft) into the ground with the required configuration that have connected to the central ground rod with #6 AWG wire according to

the lightning risk at the location and physical distribution of them (Meter Environment n.d.). In this specific case, two 2.44 m (8 ft) long copper ground rods placed between Boreholes 1&2 and Boreholes 3&4 and they connected to the central 2.44 m (8 ft) long copper ground rod next to the enclosure via #6 AWG wires as suggested. The wires in the enclosure that have connected to datalogger and multiplexers are attached to this central ground rod, as well.

CHAPTER 4. DATA COLLECTION AND RESULTS

Data Collection from Hamilton County

After sensor installation was completed, it took some time to observe and configure the data for both GS1 and MPS6 sensors. For GS1, the mV readings were out of range after sensors were connected to datalogger until mid-November. The problem with the reading may have been either caused by breakage in the data collection system that happened during the installation or unstable readings from these sensors. So, wiring and programming were checked first to solve the problem. Troubleshooting started by ensuring the connections between the wire ends and the ports physically, in case of any looseness. Then, sensor readings were examined one-by-one; first with the Procheck device, a handheld analog and digital sensor reading device compatible with all Meter Environment sensors (Figure 4.1(a)), and then with a process calibrator to read voltage outputs of the sensors (Figure 4.1(b)). The output voltage range is given as 1000 to 2500 mV in the manual and no sensor provided out of range output. Therefore, the problem for GS1s was solved by arranging the datalogger programming once more. For MPS6, 12 out of 40 sensors did not provide any output from the beginning, so this problem was investigated. They were also checked with Procheck and process calibrator, but they did not respond. Meanwhile, the vendor was informed regarding the problem, and they suggested updating sensor firmware with a file they provided. However, these sensors still did not respond.

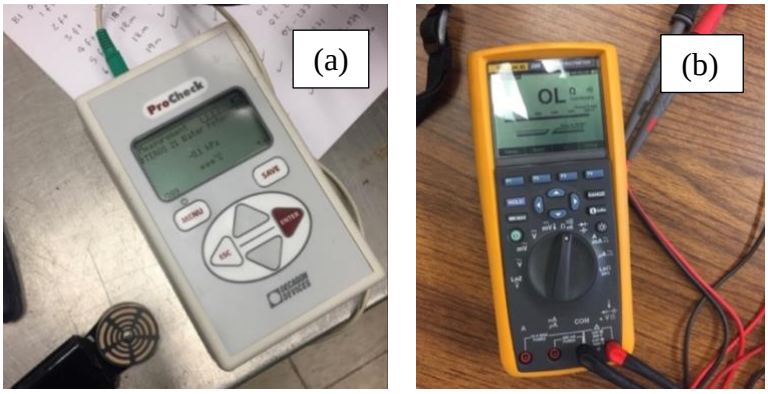

Figure 4.1 Tools used in troubleshooting: (a) Procheck, (b) Process Calibrator.

After these troubleshooting steps followed in the field and there was nothing else to do but replacing them with new sensors (12 more sensors from Meter Environment). These sensors were installed 4 ft south of the existing system on January 9th, 2019, by following the same procedure during installation (Figure 4.2). Therefore, there is missing data for the following measurement points until early January 2019: Borehole 1-0.61 m (2 ft), Borehole 1-1.83 m (6 ft), Borehole 2- 0.15 m (0.5 ft), Borehole 3-0.15 m (0.5 ft), Borehole 3-0.3 m (1 ft), Borehole 4-0.15 m (0.5 ft), Borehole 4-0.61 m (2 ft), Borehole 4-1.22 m (4 ft), Borehole 4-1.83 m (6 ft), Borehole 5-0.15 m (0.5 ft), Borehole 5-0.61 m (2 ft), Borehole 5-2.13 m (7 ft).

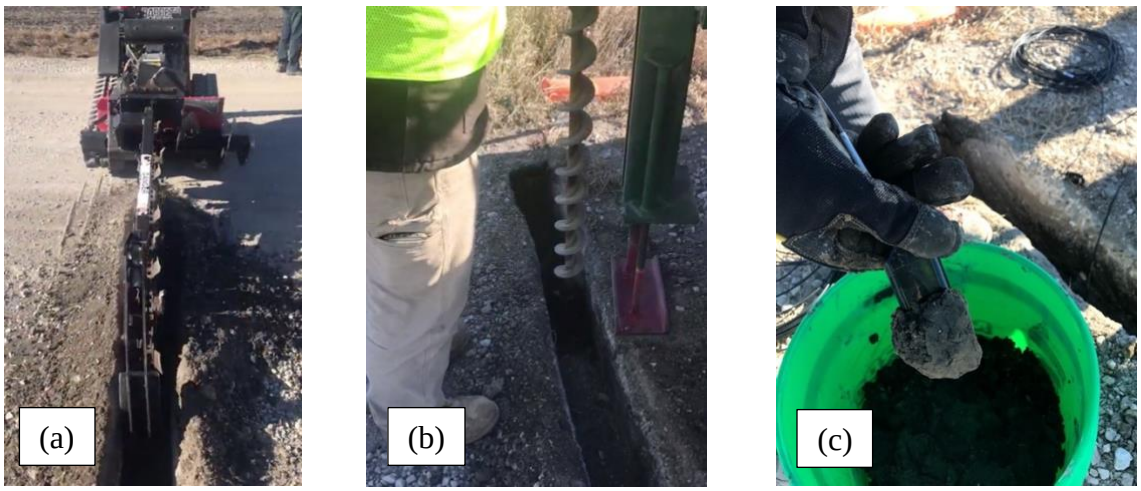

Figure 4.2 Installation of replacement sensors in January 2019: (a) digging the trench with a trencher, (b) drilling the boreholes, (c) packing MPS6 sensors with native soil.

Another data collection gaps for the MPS6 have started on January 27th, 2019 for three days and then again on January 31st, 2019 due to the "Midwest Arctic Blast"; which is the extremely cold weather conditions. The weather conditions also did not let organize the troubleshooting, so it took approximately one and a half month to solve the problem by going to the field and performing some checks.

Data collection from the weather station was only interrupted for ten days starting from early October 2018. During the installation, the plastic part attached to the U-bolt was broken so the unit was sent back for repair and we were not able to collect weather data at that time.

The collected temperature, matric potential, and water content data were grouped by their boreholes for conventional individual analyses and overlapped for periodic comparison with each other.

The top variable was selected to be the temperature due to its significance, among others. Temperature provides hints for the matric potential and water content trends by checking the phase change of the soil water. The analytical solution for determining the temperature at a certain depth and time for field applications is given as (Horton et al. 1983):

$$T(z,t) = \bar{T} + Ae^{-z\sqrt{\omega/2\alpha}} * \sin\left(\omega t - z\sqrt{\omega/2\alpha} - \phi\right) \qquad (2)$$

, where $\bar{T}$ is the average soil temperature, A is the amplitude of the surface temperature function, z is the depth from the surface level, ω is the radial frequency equals to $2\pi/P$ as P is the period of the cycle, α is the thermal diffusivity, and ϕ is the phase constant. According to this equation, the amplitude value should be decreasing as soil depth increases. Additionally, a time shift should be observed as going to deeper in the soil due to the sinusoidal properties in the equation. This suggested behavior can easily be observed in all boreholes' data (Figure 4.3 (a)).

On the other hand, matric potential and water content sensors were expected to be coherent with the temperature data and react when the temperature drops below freezing. The matric potential value tends to decrease dramatically in case of freezing especially at the temperature of 0 to -5°C and then decreases more slowly (Berg et al. 1980; Wen et al. 2012). The unfrozen soil content is very similar to matric potential behavior but drops gradually until a threshold value, which can change with initial water content (Wen et al. 2012). The drop until the threshold value happens because the sensors used in this project are capable of measuring water content by using the dielectric properties of the medium, as explained in Chapter 2 Instrumentation. However, when the water freezes and becomes ice, the dielectric property becomes smaller and undifferentiated from the dry soil conditions. Therefore, the sensors will be able to measure the unfrozen water content, which would be decreasing as soil freezes. These expected behaviors were also observed from both matric potential and water content data (Figure 4.3 (b), (c)).

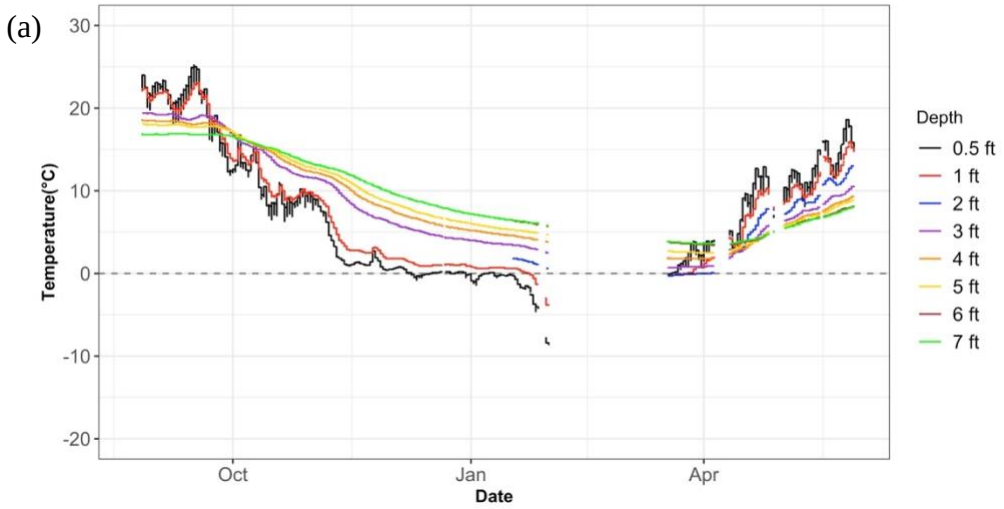

Figure 4.3 Raw data obtained from all of the sensors in Borehole 1 for: (a) Temperature, (b) Matric Potential and, (c) Volumetric Water Content.

(b)

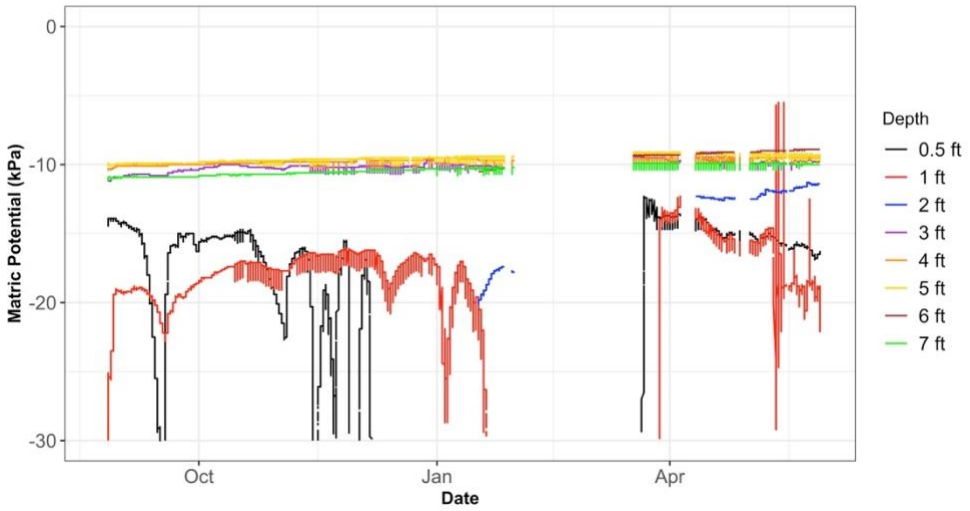

(c)

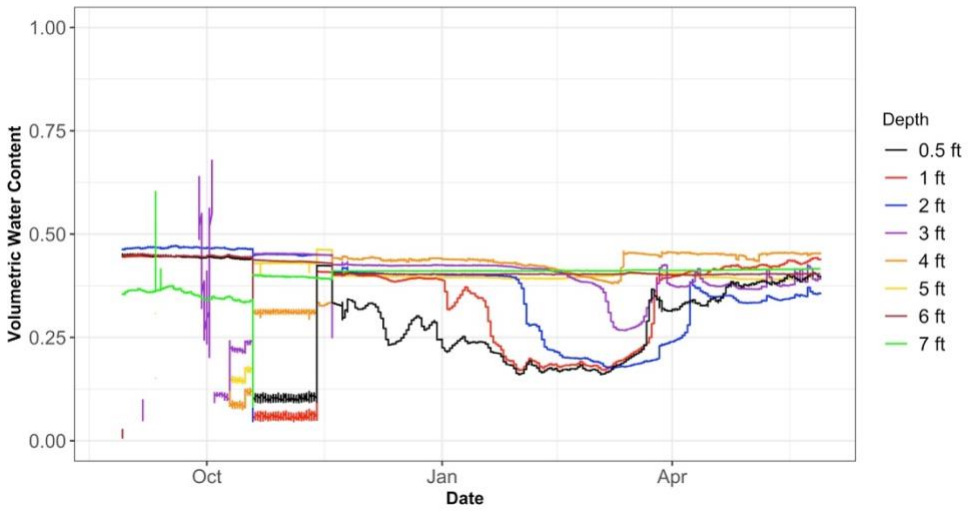

Figure 4.3 (cont.)

For freeze-thaw cycles in soil, it is assumed that the soil water has pure water properties, so it freezes at 0°C for the sake of simplicity. This assumption is made since there is no sensor or device included in the system that can detect the impurity in the soil water or the freezing point of the water.

Comparison of the Borehole Data

To make a comparison within the boreholes, three different measurements from all eight depths are grouped by their boreholes initially as stated previously. These plots were used

to examine the trends of the three parameters separately at one particular location as the depths change. For example, the temperature and matric potential data at 0.15 m (0.5 ft) and 0.30 m (1 ft) were considerably fluctuating as similar to the air temperature. However, after 0.61 m (2 ft) depth, the readings became more stable and gave their reaction to the condition change at surface later (Figure 4.4).

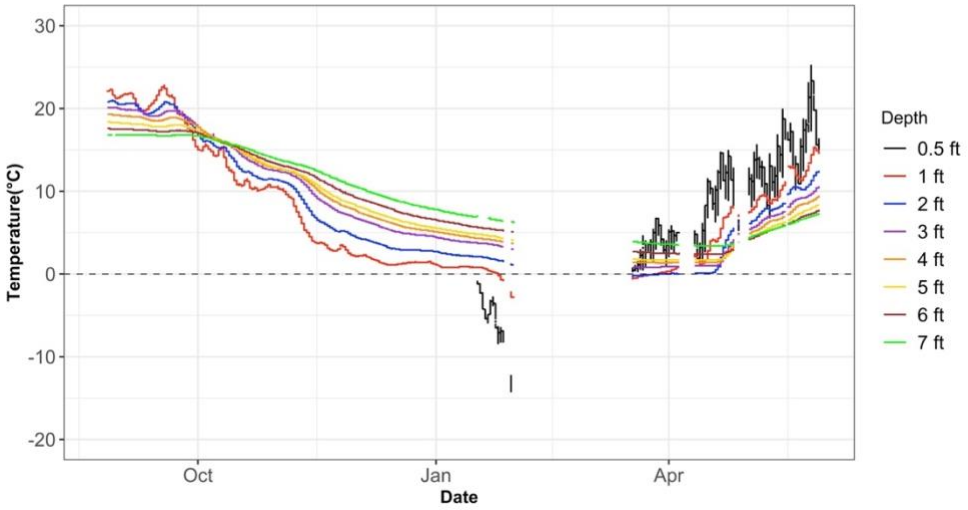

Figure 4.4 Different behavior observed from the temperature data within Borehole 2.

To accomplish an assessment between the boreholes, they were also grouped by their depths. Grouping by depths provided an overview across the road width and showed the differences in each borehole location. It was helpful to see the general trends on particular depths and compare the effect of position on the road such as shoulder vs. center or east-west. To reflect distinct changes influenced by the freeze-thaw action on the three parameters, 0.30 m, 0.91 and 2.31 m (1 ft, 3 ft and 7 ft) depths from each borehole was selected as the prominent data sets for the further discussion. These depths were selected by considering the number of working sensors throughout the time, and general fluctuation and stability characteristics on the readings.

The comparison was started with the temperature readings, which was helpful to determine whether the soil water was frozen. It would allow seeing if the matric potential and water content also indicated drier conditions (less liquid soil water) and whether it was caused by freezing of the soil water. Until May 2019, all boreholes had encountered one freeze-thaw cycle starting in January that may have reached more than 3 ft depth according to their 0°C isotherm curves created by using available temperature data.

According to the 0.30 m (1 ft) depth temperature plot, Borehole 1 and 2 that were located at the eastern side of the road started to freeze later than those of Borehole 4 and 5 on the west. The possible reason for that difference could be the difference in the sunlight (shortwave radiation/longwave radiation) exposure. However, the Borehole 3 on the center thawed first (Figure 4.5(a)). By checking the matric potential and water content plots for 0.30 m (1 ft), it was noticeable that Borehole 3 had lower water content ratio before and after freezing compared to the other boreholes (Figure 4.5(b), (c)). Soil water tends to move from warmer to the colder medium during freezing (Wen et al. 2012). That causes water content increase at that location and it can be identified with the liquid water content reading after thawing. An example of that was observed at Borehole 4 and 5, which had higher water content and they ended up being frozen the earliest. 0.30 m (1 ft) depth was the one with the most oscillating temperature data among the selected depths. It changed from -14.3°C to 25.2°C between July 2018 and May 2019. The water content values changed from 0.13 to 0.44 as freeze-thaw cycles occurred for the same borehole.

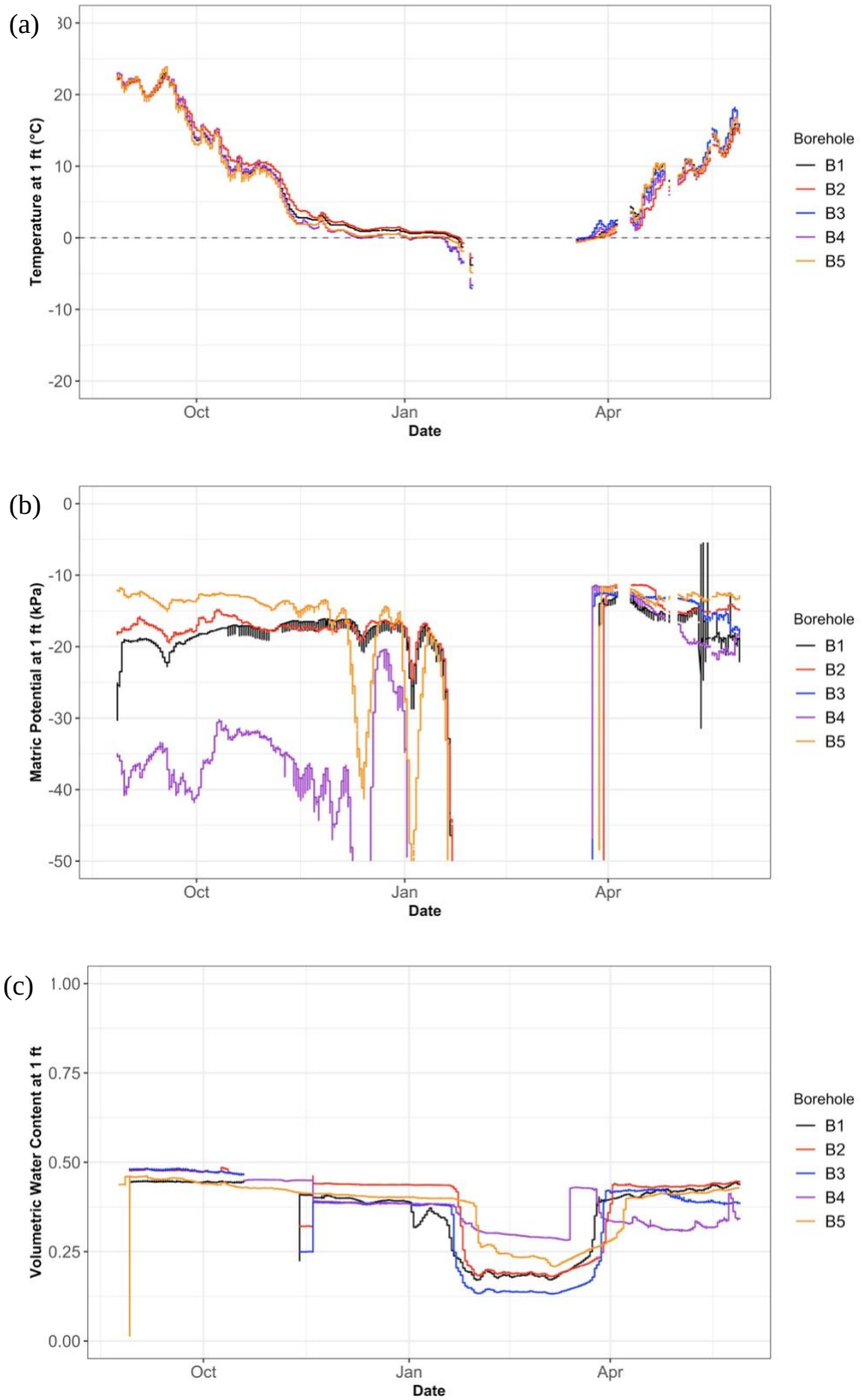

Figure 4.5 Data collected from the sensors at 30 cm (1 ft) depth from all boreholes.

The 0.91 m (3 ft) temperature data had more consistent trend overall, when compared to 0.30 m (1 ft) temperature data (Figure 4.6 (a)). The temperature values had changed from -0.2°C to 21.1°C within the collected data set, and water content from 0.20 to 0.50. Because of missing data after January, freezing behavior was difficult to interpolate by temperature. However, according to the volumetric water content data, the freezing of the soil water occurred in March with a similar order of freezing happened at 1 ft (Figure 4.6 (b),(c)).

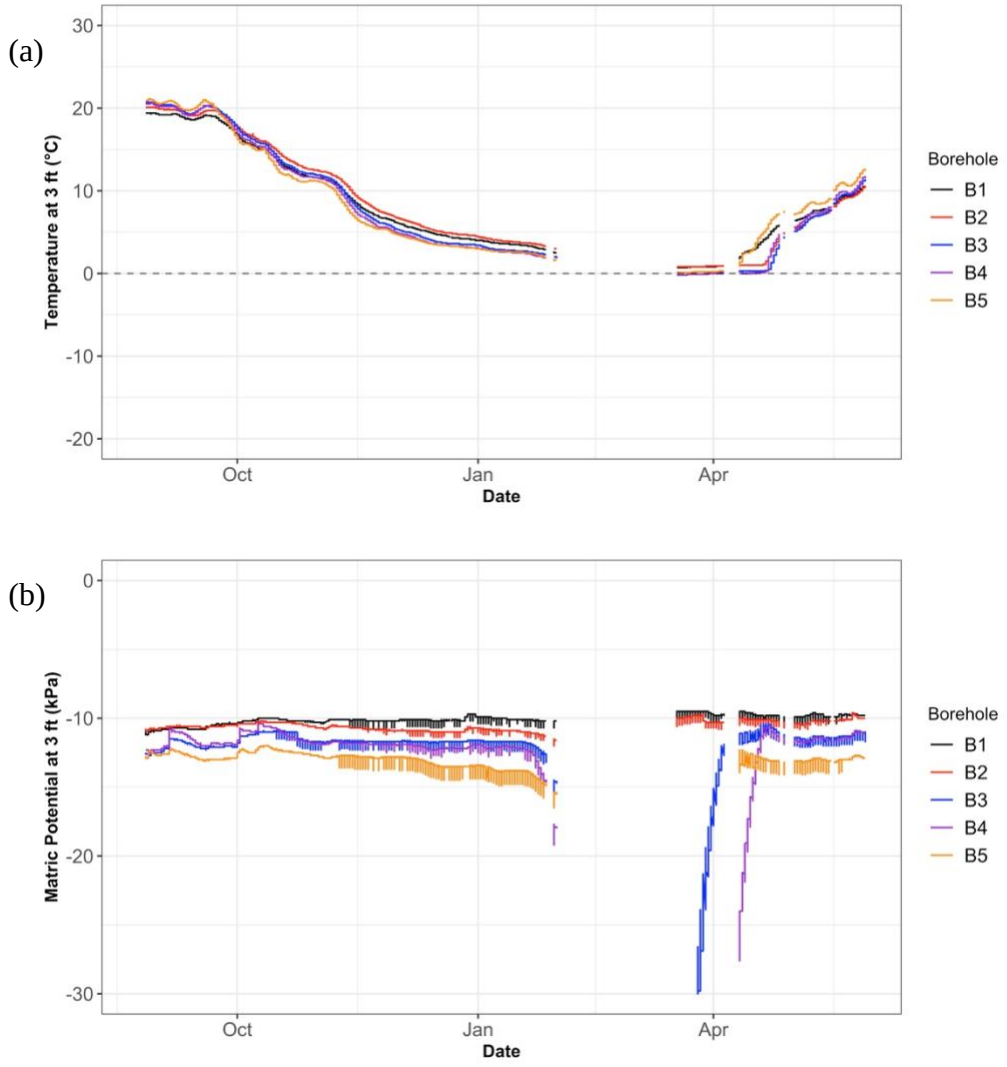

Figure 4.6 Data collected from the sensors at 0.91cm (3 ft) depth from all boreholes.

(c)

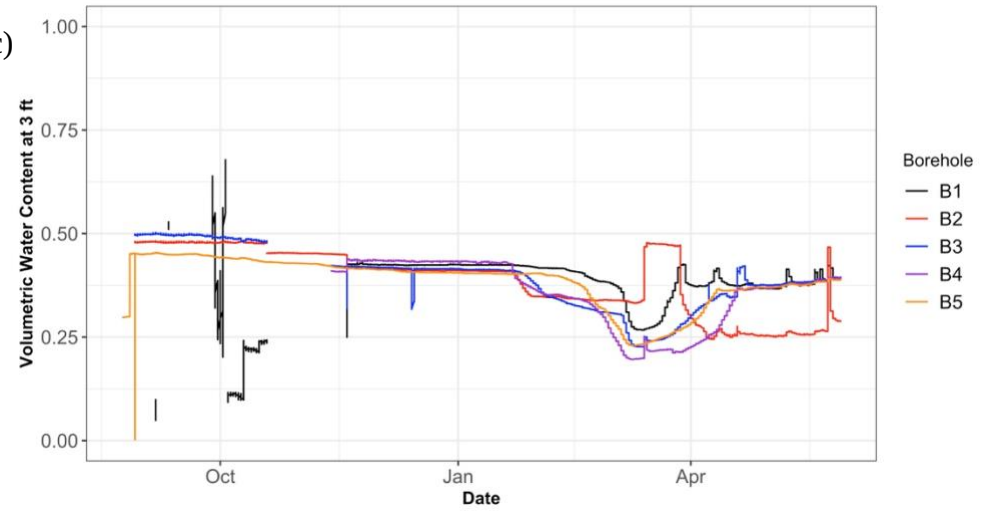

Figure 4.6 (cont.)

Finally, for the 2,13 m (7 ft) depth, which was the deepest instrumented point within this project, the trends were unchanged. The temperature responded according to the annual temperature rather than the daily changes that occurred at the surface, and it was never frozen (Figure 4.7 (a)). It changed from 3°C to 16.3°C within the data set. Therefore, the matric potential and water content levels had not changed significantly throughout the season (Figure 4.7 (b),(c)). There were some small differences between the boreholes in all of the three parameters, and it was shown that borehole 3 was the warmest among the others before freezing period started at shallower depths. This could be due to easy dissipation of the water that eventually caused drier conditions at the medium and so its temperature could change easier.

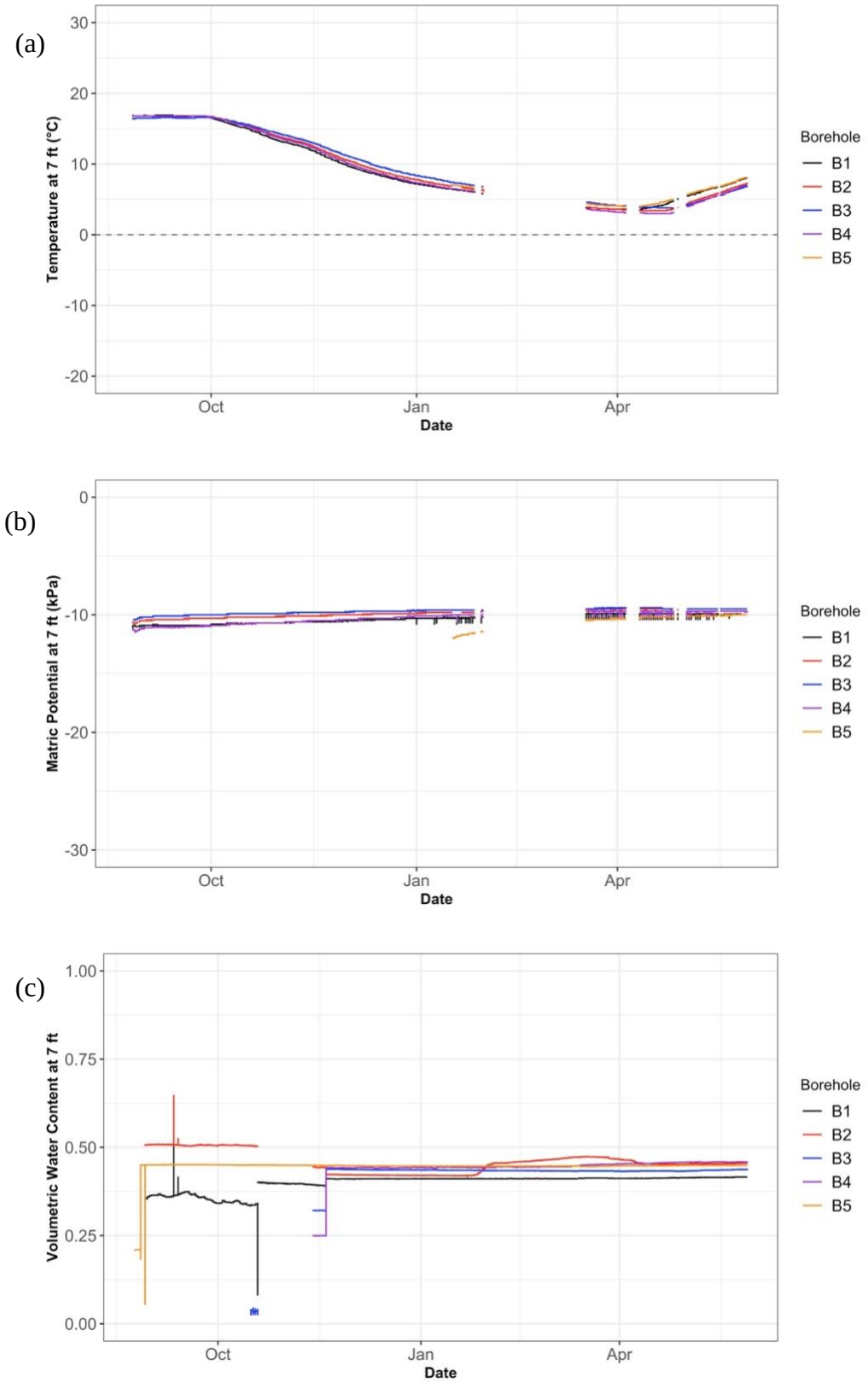

Figure 4.7 Data collected from the sensors at 2.13 cm (7 ft) depth from all boreholes.

Relationship between the Weather Data and Borehole Data

In this preliminary comparison, in addition to the previously observed freeze-thaw trends, air temperature (Figure 4.8) and precipitation (Figure 4.9) data were the keys to understand the dynamics in the borehole data. Wind speed, relative humidity, and solar radiation were the secondary parameters could be checked but mainly aimed to be used in thermal and hydraulic modeling in the future. The timeline for the borehole and weather station data were matched, and the responses in the boreholes were identified.

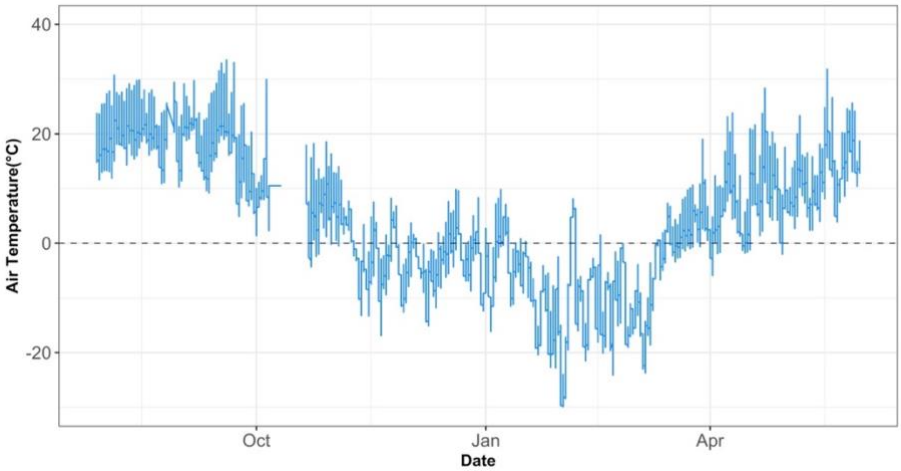

Figure 4.8 Air Temperature data of Hamilton site from ATMOS 41.

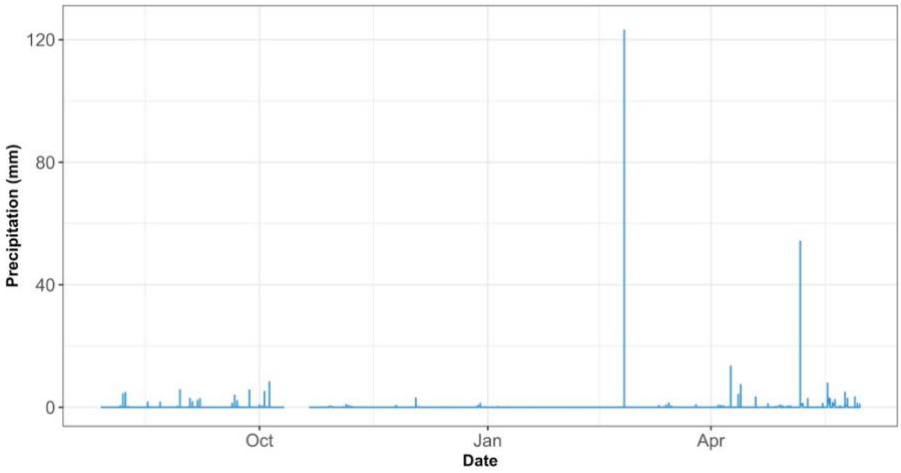

Figure 4.9 Precipitation data of Hamilton site obtained from ATMOS 41.

The 0.30 m (1 ft) data was the most susceptible to air temperature and precipitation among these three data sets compared since it was the closest to the surface level. The matric potential readings were more sensitive to the precipitation, which could be seen from the instant and noticeable increases after even light precipitation. After the heavy precipitation in May, Borehole 1 hydraulic properties had some interesting reaction. Matric potential data became unstable and oscillated, whereas water content was more stable and increased very slowly. On the other hand, water content readings demonstrated the freeze-thaw condition more clearly. However, approximately 20 days after the recorded heavy rain in late-February with 123.1 mm, the liquid water content at Borehole 4 increased suddenly, whereas other boreholes had slight increases as the water started to thaw. However, that sudden increase had decreased to 0.30-0.35 levels, when the other boreholes were at 0.40-0.43 water content level. In order to investigate the reasons of that incident, required further information regarding soil properties and profile, but it may have indicated that silty/sandy soil above 1 ft at Borehole 4 which let precipitation water to infiltrate quicker to the layers below.

For the 0.91 m (3 ft) data, the similar behavior was observed for Borehole 4 on water content plots noticed at Borehole 2 on the same dates. It increased suddenly, unlike other boreholes, and decreased dramatically to 0.25 levels. It may have been due to a similar reason or due to groundwater table fluctuations. In addition, the water content data changed as it was more sensitive to precipitation, differently than the case was noticed in 0.30 m (1 ft) data set. The matric potential data was more stable at 0.91 m (3 ft) for all boreholes. The instant increases occurred for Boreholes 3, 4 and 5, which was the similar response when soil water started to thaw, but they were not affected by the precipitation trend.

Finally, the 2.13 m (7 ft) data set was examined to see the relationship with the weather data. However, similar to the temperature data, both matric potential and water content stayed uniform throughout the season. This case indicated that neither freezing nor thawing had occurred at 2.13 m (7 ft) depth. There was only one interesting occasion at Borehole 2, which detected water content increased from 0.42 to 0.47 and decreased back gradually starting from late January until early April. However, further soil classification information was needed to identify this comparable small increase.

Comparison of Weather Station Data with Nearby RWIS Stations

As it is stated before, the purpose of the installation of a weather station is to determine whether it is sufficient to use close RWIS stations' data as inputs for the prediction models instead of constitution of a local roadside weather station at a particular location and taking the actual measurements obtained from it. For this purpose, the RWIS stations within the 48 km (30 miles) radius of the Hamilton site are found as (1) Williams – I35, (2) Iowa Falls, (3) Steamboat Rock (US20), (4) Ames(I35), and (5) Ames 6S I-35 stations. However, three of them stopped working at various dates and did not collect data since the Hamilton site was established. Thus, the remaining two RWIS stations were used for comparisons. These stations were Williams – I35 and Ames (I35).

For this study, only air temperature and wind speed data for the corresponding stations were obtained and compared with the Hamilton data by plotting them together. Air temperature of both RWIS stations followed the same trend as observed in Hamilton (Figure 4.10(a)). Ames usually went through higher temperature values than Hamilton, whereas Williams was generally lower. This trend was expected since Ames is located at the south of Hamilton and Williams is in the north. Besides, the maximum difference between RWIS stations and Hamilton was not more than 5°C. On the other hand, wind speed at Williams was usually

higher than the others and data was more variable among these three (Figure 4.10 (b)). Further statistical analyses are needed for more detailed evaluation.

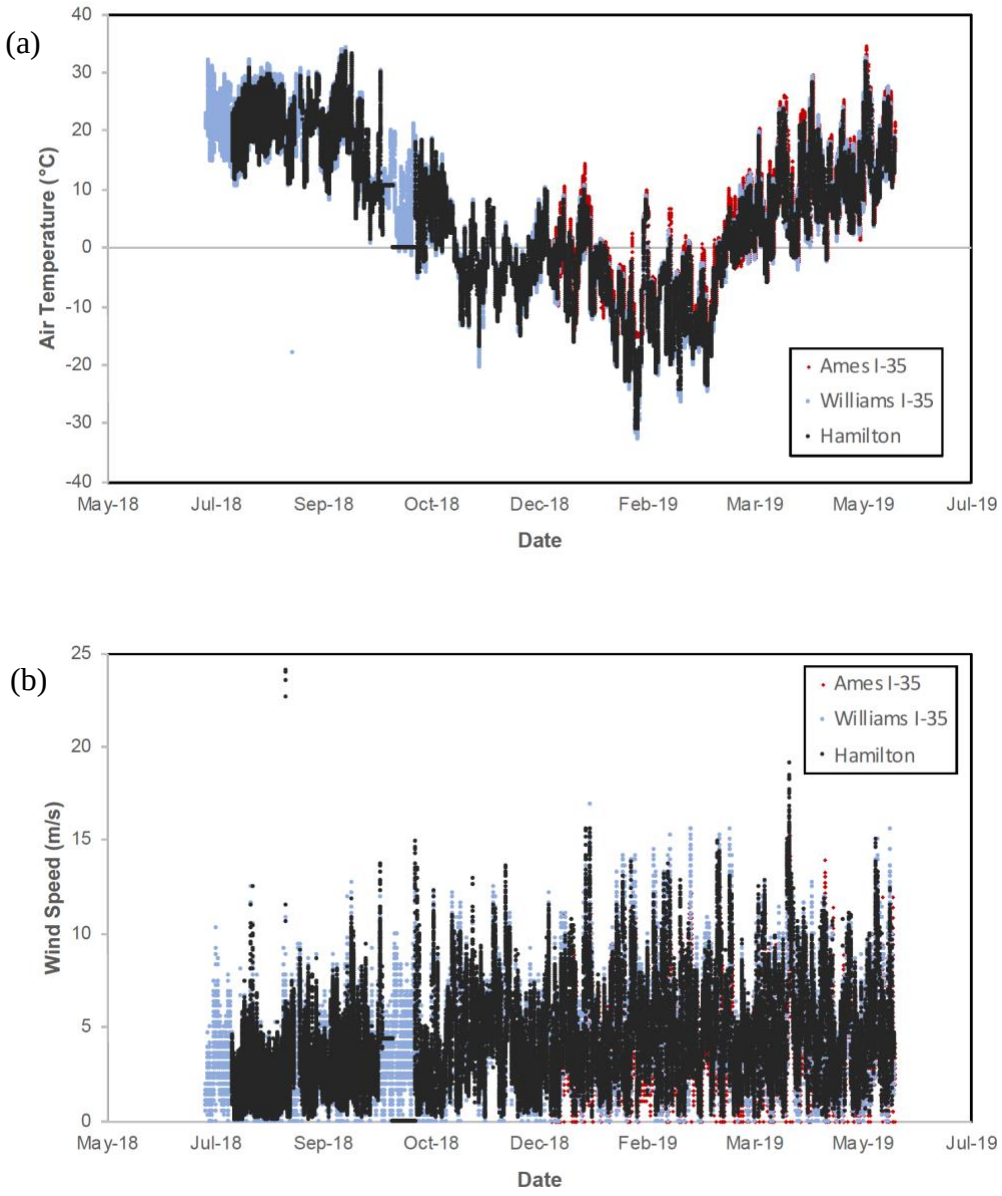

Figure 4.10 Comparison of (a) air temperature, and (b) wind speed data obtained from weather station with near RWIS measurements.

CHAPTER 5. CONCLUSIONS AND RECOMMENDATIONS

Conclusions

Field monitoring experiments are very valuable in geotechnical engineering due to soil's heterogeneous structure. Soil behavior is affected significantly by weather conditions and water presence. In addition, the design and development of such monitoring systems require careful pre-planning and applications, especially if long-term functioning is necessary. The design and installation experiences in a relatively complicated monitoring system are shared in this thesis to help future researchers to create more efficient implementations.

The instrumentation and installation procedures should be organized beforehand by anticipating possible difficulties and challenges in the application and manage the courses of actions accordingly. Even though all of the steps planned before, the researchers should be ready for unexpected challenges after the installation is completed. Severe weather, unstable data reading, or even sensor shut down are still a possibility which can affect the monitoring quality. Identifying the troubleshooting steps clearly in case of a problem and facilitating vendor-researcher communication can accelerate the procedure.

Collected data can be analyzed in various ways. In this study, data were categorized by their boreholes to investigate the changes in a particular location, and by their depths to explore the effect of position. Temperature data showed clearly the expected trend, where the amplitude of the temperature function decreased, and temperature changes delayed as depth increased. Matric potential and volumetric water content measurements were coherent with the temperature data and decreased suddenly during freezing started as expected.

However, there were some differences in the values causing unsymmetrical response for different boreholes. The possible reasons for these dissimilar results are uneven conditions

such as actual aggregate layer thicknesses that water penetrates, unpredictable water discharges, uneven precipitation, sunlight, and traffic load exposures. Besides, laboratory analyses regarding soil classification would be helpful to understand their effect on these smaller fluctuations at different locations.

For the matric potential sensors, no significant variations were observed between the vertical and horizontal orientations in the raw data other than what was discussed in the Results section for sensors at different locations and depths. Therefore, the simpler vertical orientation is recommended for the installation of MPS6 sensor. Finally, RWIS stations within 48 km (30-miles) radius provided similar structure with data obtained from Hamilton test site. However, further statistical analyses would be helpful for further evaluations and especially in the case of using in a freeze-thaw prediction model.

Recommendations

After this installation experience, many important lessons learned that it is worth to share. First of all, possible location shifts should be the cable length calculations by adding more extra length, within the convenience of budget. In this installation, 90 cm (3 ft) of extra is added each sensor cable. Yet some of the sensors, mostly from the Borehole 1 and 2, could not reach to the datalogger or multiplexer ports they supposed to, so the short cables were spliced by using the extension of other cables by following the vendor's suggested procedure (Meter Environment n.d.)(Figure 5.1). This shortage happened due to the few centimeters shift on the boreholes' plane during installation that supposed to be aligned with the enclosure. So, the extra length should be estimated by considering these possible changes and structure of the site.

Figure 5.1 Cable splicing for the short cables.

In large sensor network installations, as presented herein, the sensor pre-checks become valuable to avoid any complications in the field. In this case, 12 matric potential/temperature sensors were unresponsive despite comprehensive troubleshooting. The field conditions also do not always provide the most suitable troubleshooting conditions with unsuitable weather conditions or limited available space. Therefore, both laboratory and field trials of the entire data acquisition system and all sensors are recommended in order to avoid similar problems. For this particular case; Procheck, a compact sensor reading device from Meter Environment, is very helpful to conduct the primary examinations.

During the installation of sensors at deeper locations such as 1.52, 1.83 and 2.13 m (5, 6 and 7 ft) deep; groundwater level restrained successful application. An existing water bottle was used at first to drain some of the water, but it was not successful at all. Next, a small utility pump powered by a truck's battery was used, but it could not provide the intended conditions, either. Thus, depending on the local groundwater table level, a stronger utility pump with the ability to pump faster and deeper should be brought to the site.

Furthermore, the PVC conduit underneath the cross-section was placed approximately 5 cm (2 inches) under the aggregate layer. This distance could be extended to 10 cm (4 inches) or deeper to ensure the long-term survival of the PVC and the cables passing inside.

Last but not least, some native soil samples should be collected during the drilling. These samples should be stored in sealed bags to conduct water content measurement and soil classification tests in the laboratory or perform further soil-specific calibration process for the sensors. Water content measurements would be beneficial to compare the actual water content levels to the sensor readings.

REFERENCES

Albers, J. (2017). "How Much Power Does Your Data Acquisition System Need?" *Campbell Scientific*, <https://www.campbellsci.com/blog/power-for-data-acquisition-system> (Nov. 8, 2018).

Baker, T. H. W., Davis, J. L., Hayhoe, H., and Topp, G. C. (1982). "Locating the frozen-unfrozen interface in soils using time-domain reflectometry." *Canadian Geotechnical Journal*, 19, 511–517.

Beckemeyer, C. A. (2015). "Virtual RWIS : Reducing Costs with Real-Time Roadway Weather Information." *IBTTA 2015 Maintenance & Roadway Operations Workshop*, Applied Research Associates, Inc., 1–18.

Berg, R., Ingersoll, J., and Guymon, G. (1980). "Frost heave in an instrumented soil column." *Cold Regions Science and Technology*, 3(2–3), 211–221.

Bittelli, M. (2011). "Measuring Soil Water Content: A Review." *Improvement in Nitrogen and Water Use Efficiency: Interest of Assessment Tools*, Hort Technology, Bologna.

Campbell Scientific. (2014). "Power Budget Spreadsheet." <https://www.campbellsci.com/downloads/power-budget-spreadsheet>.

Campbell Scientific. (2019a). "PC400 Datalogger Support Software." <https://www.campbellsci.com/pc400>.

Campbell Scientific. (2019b). "Product Manual CR1000X Measurement and Control Datalogger." Campbell Scientific.

Campbell Scientific. (2019c). "Product Manual AM16/32B Relay Multiplexer." Campbell Scientific.

Cassel, D. K., and Klute, A. (1986). "Water Potential : Tensiometry." *Methods of Soil Analysis, Part 1. Physical and Mineralogical Methods*, A. Klute, ed., American Society of Agronomy - Soil Science Society of America, Madison, Wisconsin.

Cheng, Q., Sun, Y., Jones, S. B., Vasilyev, V. I., Popov, V. V., Wang, G., and Zheng, L. (2014). "In situ measured and simulated seasonal freeze-thaw cycle: A 2-year comparative study between layered and homogeneous field soil profiles." *Journal of Hydrology*, Elsevier B.V., 519(PB), 1466–1473.

Cobos, D. (2019). "Soil Water Potential Measurement." Decagon Devices and Washington State University.

Decagon Devices. (2015a). *GS1 Soil Moisture Sensor Operator's Manual*. Decagon Devices, Inc., Pullman, WA.

Decagon Devices. (2015b). “Dielectric Water Potential Sensors Operator’s Manual.” Decagon Devices, Inc., Pullman, WA.

Evett, S. R., Tolk, J. A., and Howell, T. A. (2006). “Soil Profile Water Content Determination: Sensor Accuracy, Axial Response, Calibration, Temperature Dependence, and Precision.” *Vadose Zone Journal*, 5, 894–907.

Ewan, L., and Al-Kaisy, A. (2017). *Assessment of Montana Road Weather Information System (RWIS)*. Bozeman.

Ferré, P. A., and Topp, G. C. (2000). “Time-domain Reflectometry Techniques for Soil Water Content and Electrical Conductivity Measurements.” *Sensors Update*, 7(1), 277–300.

Hallikainen, M. T., Ulaby, F. T., Dobson, M. C., El-Rayes, M. A., and Wu, L.-K. (1985). “Microwave Dielectric Behavior of Wet Soil-Part I: Empirical models.” *IEEE Transactions on Geoscience and Remote Sensing*, GE-23(1), 25–34.

He, H., Dyck, M. F., Si, B. C., Zhang, T., Lv, J., and Wang, J. (2015). “Soil freezing-thawing characteristics and snowmelt infiltration in Cryalfs of Alberta, Canada.” *Geoderma Regional*, Elsevier B.V., 5, 198–208.

Heitman, J. L., Horton, R., Ren, T., Nassar, I. N., and Davis, D. D. (2008). “A Test of Coupled Soil Heat and Water Transfer Prediction under Transient Boundary Temperatures.” *Soil Science Society of America Journal*, 72(5), 1197.

Heitman, J. L., Zhang, X., Xiao, X., Ren, T., and Horton, R. (2017). “Advances in Heat-Pulse Methods: Measuring Soil Water Evaporation with Sensible Heat Balance.” *Methods of Soil Analysis*, 2(1), 0.

Hillel, D. (2004). *Introduction to Environmental Soil Physics*. Elsevier Academic Press.

Horton, R., Wierenga, P. J., and Nielsen, D. R. (1983). “Evaluation of Methods for Determining the Apparent Thermal Diffusivity of Soil Near the Surface1.” *Soil Science Society of America Journal*.

Huisman, J. A., Hubbard, S. S., Redman, J. D., and Annan, A. P. (2003). “Measuring Soil Water Content with Ground Penetrating Radar : A Review.” *Vadose Zone Journal*, 2(4), 476–491.

Incropera, F. P., Dewitt, D. P., Bergman, T. L., and Lavine, A. S. (2007). *Fundamentals of Heat and Mass Transfer*. John Wiley & Sons, Inc., Hoboken, NJ.

Iowa County Engineers Association. (2019). “About Secondary Roads.”

Jury, W. A., and Horton, R. (2004). *Soil Physics*. John Wiley & Sons, Inc., New Jersey.

Kang, Y., Liu, Q., and Huang, S. (2013). "A fully coupled thermo-hydro-mechanical model for rock mass under freezing/thawing condition." *Cold Regions Science and Technology*, Elsevier B.V., 95, 19–26.

Kelleners, T. J., Robinson, D. A., Shouse, P. J., Ayars, J. E., and Skaggs, T. H. (2005). "Frequency Dependence of the Complex Permittivity and Its Impact on Dielectric Sensor Calibration in Soils." *Soil Science Society of America Journal*, 69(1).

Konrad, J.-M., and Morgenstern, N. R. (1980). "A mechanistic theory of ice lens formation in fine-grained soils." *Canadian Geotechnical Journal*, 17(4), 473–486.

Konrad, J. M. (1989). "Physical processes during freeze-thaw cycles in clayey silts." *Cold Regions Science and Technology*, 16(3), 291–303.

Körschens, M. (2006). "The importance of long-term field experiments for soil science and environmental research - a review." *Plant Soil Environement*, 52, 1–8.

Kwon, T. J., Fu, L., and Jiang, C. (2015). "Road weather information system stations — where and how many to install: a cost benefit analysis approach." *Canadian Journal of Civil Engineering*, 42, 57–66.

Liu, G., Wen, M., Chang, X., Ren, T., and Horton, R. (2013). "A Self-Calibrated Dual Probe Heat Pulse Sensor for In Situ Calibrating the Probe Spacing." *Soil Science Society of America Journal*, 77, 417–421.

Manfredi, J., Walters, T., Wilke, G., Osborne, L., Hart, R., Incrocci, T., and Schmitt, T. (2005). *Road Weather Information System Environmental Sensor Station Siting Guidelines*. *Animal Genetics*.

Manfredi, J., Walters, T., Wilke, G., Osborne, L., Hart, R., Incrocci, T., Schmitt, T., Garrett, V. K., Boyce, B., and Krechmer, D. (2008). *Road Weather Information System Environmental Sensor Station Siting Guidelines, Version 2.0*. Washington, DC.

Meter Environment. (n.d.). "Lightning surge and grounding practices." <https://www.metergroup.com/environment/articles/lightning-surge-grounding-practices/>.

Meter Environment. (n.d.). "Wire splicing and sealing technique for soil moisture sensors." <https://www.metergroup.com/environment/articles/wire-splicing-sealing-technique-soil-moisture-sensors/>.

Milly, P. C. D. (1980). "The Coupled Transport Water Heat Vertical Soil Column Under Atmospheric Excitation.Pdf." Massachusetts Institite of Technology.

Milly, P. C. D. (1982). "Moisture and heat transport in hysteretic, inhomogeneous porous media: A matric-head based formulation and a numerical model." *Water Resources Research*, 18(3), 489–498.

Mittelbach, H., Lehner, I., and Seneviratne, S. I. (2012). "Comparison of four soil moisture sensor types under field conditions in Switzerland." *Journal of Hydrology*, Elsevier B.V., (430–431), 39–49.

Nassar, I. N., and Horton, R. (1992). "Simultaneous Transfer of Heat, Water, and Solute in Porous Media: I. Theoretical Development." *Soil Science Society of America Journal*, 56, 1350–1356.

Nassar, I. N., and Horton, R. (1997). "Heat, Water, and Solute Transfer in Unsaturated Porous Media: I - Theory Development and Transport Coefficient Evaluation." *Transport in Porous Media*, 27(1), 17–38.

Orr, D., Kestler, M., Andersen, T., and Larson, G. (2017). *Springtime Damage to roads and Seasonal Load Limits [Webinar]*.

Overduin, P. P., Kane, D. L., and van Loon, W. K. P. (2006). "Measuring thermal conductivity in freezing and thawing soil using the soil temperature response to heating." *Cold Regions Science and Technology*, 45(1), 8–22.

Ovik, J. M., Siekmeier, J. A., and Van Deusen, D. A. (2000). *Improved Spring Load Restriction Guidelines Using M Analysis-MNDOT*. St. Pauls.

Parsons Brinckerhoff, and Iteris. (2013). *Road Weather Information System (RWIS) Evaluation Technology Evaluation Memorandum*.

Peng, X., Wang, Y., Heitman, J., Ochsner, T., Horton, R., and Ren, T. (2017). "Measurement of soil-surface heat flux with a multi-needle heat-pulse probe." *European Journal of Soil Science*, 68, 336–344.

Philip, J. R., and De Vries, D. A. (1957). "Moisture movement in porous materials under temperature gradients." *Transactions, American Geophysical Union*, 38(2), 222–232.

Robinson, D. A., Jones, S. B., Wraith, J. M., Or, D., and Friedman, S. P. (2003). "A Review of Advances in Dielectric and Electrical Conductivity Measurement in Soils." *Vadose Zone Journal*, 2, 444–475.

Saarenketo, T., and Aho, S. (2005). *Managing Spring Thaw Weakening on Low Volume Roads*.

SDI-12 Support Group. (n.d.). "Serial Digital Interface at 1200 Baud." <http://sdi-12.org>.

SDI-12 Support Group. (2019). "SDI-12 A Serial-Digital Interface Standard for Microprocessor-Based Sensors." *SDI-12 Support Group*, SDI-12 Support Group, River Heights, Utah.

Seyfried, M. S., and Murdock, M. D. (2004). "Measurement of Soil Water Content with a 50-MHz Soil Dielectric Sensor." *Soil Science Society of America Journal*, 68(2).

Sophocleous, M. (1979). “Analysis of Water and Heat Flow in Unsaturated-Saturated Porous Media.” *Water Resources Research*, 15(5), 1195–1206.

Spaans, E. J. A., and Baker, J. M. (1996). “Soil Freezing Characteristic: Its Measurement and Similarity to the Soil Moisture Characteristic.” *Soil Science Society of America Journal*, 60, 13–19.

Sun, Y., Cheng, Q., Xue, X., Fu, L., Chai, J., Meng, F., Schulze Lammers, P., and Jones, S. B. (2012). “Determining in-situ soil freeze-thaw cycle dynamics using an access tube-based dielectric sensor.” *Geoderma*, 189–190, 321–327.

Topp, G. C. (2003). “State of the art of measuring soil water content.” *Hydrological Processes*, 17, 2993–2996.

Topp, G. C., Davis, J. L., and Annan, A. P. (1980). “Electromagnetic Determination of Soil Water Content:” *Water Resources Research*, 16(3), 574–582.

Topp, G. C., Parkin, G. W., and Ferré, T. P. A. (2008). “Soil Water Content.” *Soil Sampling and Methods of Analysis*, M. R. Carter and E. G. Gregorich, eds., CRC Press, 939–961.

Vavrik, W. R., Dwyer, C. E., Brink, W. C., Larson, G., and Applied Research Associates, I. (2016). *Evaluation of Software Simulation of Road Weather Information System*. *Civil Engineering Studies, Illinois Center for Transportation Series*.

Wang, D. yan, Ma, W., Niu, Y. hong, Chang, X. xiao, and Wen, Z. (2007). “Effects of cyclic freezing and thawing on mechanical properties of Qinghai-Tibet clay.” *Cold Regions Science and Technology*, 48(1), 34–43.

Wen, Z., Ma, W., Feng, W., Deng, Y., Wang, D., Fan, Z., and Zhou, C. (2012). “Experimental study on unfrozen water content and soil matric potential of Qinghai-Tibetan silty clay.” *Environmental Earth Sciences*, 66(5), 1467–1476.

Xu, J., Ma, X., Logsdon, S. D., and Horton, R. (2011). “Short, Multineedle Frequency Domain Reflectometry Sensor Suitable for Measuring Soil Water Content.” *Soil Science Society of America Journal*, 76, 1929–1937.

Zapata, C., and Houston, W. (2008). *Calibration and Validation of the Enhanced Integrated Climatic Model (EICM) for Pavement Design*. Tempe, AZ.

Zhang, S., Teng, J., He, Z., and Sheng, D. (2016). “Importance of vapor flow in unsaturated freezing soil: A numerical study.” *Cold Regions Science and Technology*, Elsevier B.V., 126, 1–9.